Applied Catalysis B: Environmental 176–177 (2015) 20–35

Contents lists available at ScienceDirect

Applied Catalysis B: Environmental

journal homepage: www.elsevier.com/locate/apcatb

# Towards carbon efficient biorefining: Multifunctional mesoporous solid acids obtained from biodiesel production wastes for biomass conversion

Lakhya Jyoti Konwar[a,b,1], Päivi Mäki-Arvela[b], Eero Salminen[b], Narendra Kumar[b], Ashim Jyoti Thakur[c], Jyri-Pekka Mikkola[b,d,*], Dhanapati Deka[a]

[a] Biomass Conversion Laboratory, Department of Energy, Tezpur University, Tezpur 784028, Assam, India
[b] Laboratory of Industrial Chemistry and Reaction Engineering, Process Chemistry Centre, Åbo Akademi University, FI-20500, Finland
[c] Department of Chemical Sciences, Tezpur University, Tezpur 784028, Assam, India
[d] Technical Chemistry, Department of Chemistry, Chemical–Biological Centre, Umeå University, SE-901 87 Umeå, Sweden

ARTICLE INFO

*Article history:*
Received 20 January 2015
Received in revised form 1 March 2015
Accepted 5 March 2015
Available online 24 March 2015

*Keywords:*
Sulfonated carbons
Biorefining
Catalyst characterization
De-oiled waste cake
Biodiesel
Esterification
Reducing sugars

ABSTRACT

Multifunctional mesoporous solid acids were prepared by the sulfonation of carbonized de-oiled seed waste cake (DOWC), a solid waste from biodiesel production. Detailed structural characterization of the materials by elemental analysis, FT-IR, Raman, XRD, XPS, TGA, $NH_3$-TPD and $N_2$-physisorption showed that they were structurally different from the carbohydrate and resin based sulfonated carbon catalysts. In addition to the typical —OH, —COOH and —$SO_3H$ groups they contain several N species (pyridinic, pyrrolic etc.) incorporated in their carbon frameworks. The basic structural unit of these materials is a flexible carbon nitride sheet which is extensively functionalized with acidic groups. Our results show distinct effects of raw material composition and preparation methods (activation, sulfonating agent etc.) on structure, stability, surface acidity and textural properties. Here, catalyst —$SO_3H$ density and porosity (pore size, pore volume and surface area) had a direct effect on activity. Also, $H_2SO_4$ was less useful than 4-BDS (4-benzenediazoniumsulfoante) as a sulfonating agent. The best catalysts with mesoporous structure (average pore diameter 3.9–4.8 nm, pore volume 0.28–0.46 $cm^3\ g^{-1}$) and —$SO_3H$ density (0.70–0.84 $mmol/g_{cat}$) were obtained by 4-BDS sulfonation of chemically activated DOWCs. In contrast, hydrothermal $H_2SO_4$ sulfonation of DOWC produced a non-porous catalyst with high —$SO_3H$ density while those obtained by $H_2SO_4$ treatment of activated biomass (AC) had a porous structure with low —$SO_3H$ density (0.19 $mmol/g_{cat}$). Furthermore, the reported catalysts show excellent activity in two reactions of interest in biomass conversion: cellulose saccharification (glucose yield 35–53%) and fatty acid esterification (conversion upto 97%) outperforming $H_2SO_4$, conventional solid acids (zeolites, ion-exchange resins etc.) as well as sulfonated carbons reported earlier works, confirming their potential as alternative environmentally benign solid catalysts for sustainable, carbon efficient biorefining.



## 1. Introduction

Due to the growing energy crisis and environmental concerns utilization of renewable resources for the production of fuels and chemicals has recently attracted a lot of attention. Thus the conversion of biomass and the platform molecules derived from it into more sustainable bio-based fuels and chemicals (biorefining), is of great interest. Biofuels such as biodiesel and bioalcohols (bioethanol/biobutanol) are presently considered the best alternatives to fossil based liquid fuels [1]. Vegetable oils, fats and fatty acids are the most common feedstock used for biodiesel production while bioalcohols are produced from starchy as well as lignocellulosic biomass. It is a well accepted fact that next to feedstock, catalyst plays the most important role in any chemical transformation by affecting the overall process economics and product costs. Indeed, catalysis is considered as a key, enabling technology for the development of competitive, carbon efficient biorefineries. The current generation technology for biomass conversion still relies on

* Corresponding author at: Laboratory of Industrial Chemistry and Reaction Engineering, Process Chemistry Centre, Åbo Akademi University, FI-20500, Finland. Tel.: +358 22154574.
*E-mail addresses:* lakhya07@gmail.com (L.J. Konwar), jpmikkol@abo.fi (J.-P. Mikkola).
[1] Tel.: +91 9707607641; fax: +91 3712 267005/6

http://dx.doi.org/10.1016/j.apcatb.2015.03.005
0926-3373/

the use of homogenous acids such as HCl, $H_2SO_4$ as catalyst during many transformation steps, a major hurdle in their large scale commercialization [2]. In recent years, within the emerging concepts of green chemistry use of eco-friendly materials and bio-inspired catalysts for chemical transformations has gained immense attention [3–5]. Among these, the sulfonated carbons have emerged out as promising solid acid and substitute to sulfuric acid. They are a new class of promising, diverse novel solid catalysts active in a range of acid catalyzed reactions including reactions of importance in biomass conversion (biorefining): esterification, transesterification (biodiesel production) [4,5] cellulose saccharification (bioalcohol production and biorefining) [5], glycerol etherification (diesel additive) [6] and to name others. They demonstrate ideal catalytic features such as high mechanical, thermal and chemical stability, water tolerance, activity and low material cost. Over the years, although a large number of manuscripts detailing preparation and applications of these sulfonic acid functionalized materials have been reported. The preparation has been seldom based on a method pioneered by Hara et al. [4] involving sulfonation of an incompletely pyrolysed carbonaceous material obtained from sources such as: sucrose [7], glucose [4,8], starch [9], glycerol [10], biochar [11], wood [12], oil pitch [13], canola meal [14], corncob [15] and to name others. Similar, catalysts have also been prepared from more expensive carbon precursors such as phenolic resins [16], carbon foams [17] graphene [18] and OMCs [19,20]. However, considering that biomass is renewable, abundant and low-cost, sulfonated carbons produced directly from biomass and bio-wastes has potential advantage. In brief, in the majority of studies to obtain sulfonated carbons, the carbon precursors were directly pyrolyzed and treated with strong sulfonating agents (conc. $H_2SO_4$ or fuming $H_2SO_4$, except Refs. [17,19,20]) at high temperature. But since the sulfonation step is carried out with large amounts of concentrated acids at a high temperature (150–250 °C), the process may not be reasonably called an eco-friendly. In addition, $H_2SO_4$ is reported to be ineffective for sulfonating aromatized, ordered and rigid carbon materials such as graphite, activated carbons (AC) or carbons prepared by high temperature treatment [4,5,8,9,14,15]. Hence, by applying the conventional $H_2SO_4$ sulfonation it is very difficult to sulfonate ACs, in other words to prepare catalysts simultaneously possessing high porosity (large pore size, pore volume, specific surface area) and $-SO_3H$ density, vital features when considering catalytic applications in conversion of large biomass molecules. Recently, it has been demonstrated that sulfonation could be more effective using 4-BDS (4-benzenediazoniumsulfonate radicals) instead of $H_2SO_4$ due to use of mild conditions, preservation of structural, morphological features of support and the capacity to sulfonate more rigid and ordered carbon structures (AC, graphene, OMC etc.). This approach has been found particularly helpful for sulfonating highly ordered and aromatized carbon materials (e.g., graphene, OMC, AC) and prepare sulfonated carbon catalysts that simultaneously exhibit high porosity and acid exchange capacity. Typically, the porous sulfonated carbon materials are prepared via multi-steps and high-cost strategy, usually involving sulfonation of OMC prepared by a template method [19,20]. In contrast the use of biomass derived porous AC supports for sulfonation is economically more attractive. Although several articles dealing with the preparation of sulfonated carbons from different waste sources could be found in open literature, there are virtually no reports on the employment of end wastes from biodiesel production for making carbon based catalysts. Similarly, studies investigating the effects of preparation method (activation, sulfonating agent etc.), raw material properties on catalyst structure and activity are in lack [17,19,20].

With the growing biodiesel market the use of oil from non-edible seeds such as *Jatropha curcas*, *Ricinus communis* (Castor) and *Pongamia pinnata* has increased in recent years. Oil processing from such seeds generates large quantities of solid wastes in the form of seed hulls and de-oiled waste cake (DOWC). DOWC is an end waste commonly associated with non-edible seeds processing (biodiesel production). Albeit a good source of protein, when obtained from non-edible seeds these cakes do not posses any direct nutritional value as food or fertilize source due to the presence of various anti-nutritional, toxic components (phorbol ester, ricin, karanjin etc.). For the same reason and the low carbohydrate contents they are also not suitable as a feedstock for bioalcohol production or for conversion into manure or direct burning [21–23]. On the other hand, controlled thermochemical conversion of DOWC biomass has been identified to produce high value co-products such as activated carbon (AC), biochar, bio-oil, charcoal for use in the non-food sector [22,23]. Utilization of agricultural residues for preparing AC has already been identified as a cost effective method for waste disposal [24]; extending this concept to the DOWC may be an efficient solution for dealing with these wastes, considering large market opportunities for AC and also from the possible application of such materials during biodiesel production as catalyst, adsorbent for oil,

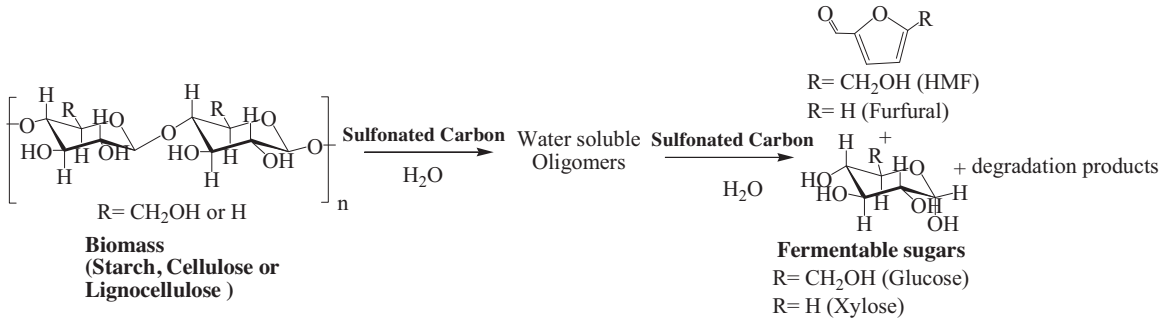


**Scheme 1.** Hydrolysis of cellulose/biomass.

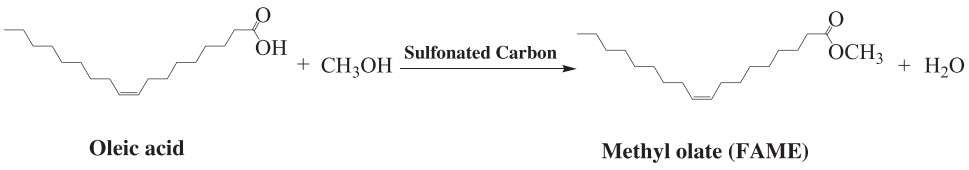


**Scheme 2.** Esterification of oleic acids with methanol.

or in waste water treatment. Besides, the integration of carbon catalyst generated from biodiesel wastes would not only resolve a major waste disposal issue but also contribute to higher carbon efficiencies through better utilization of starting biomass leading to reduce biodiesel prices.

The present study builds on our earlier work which has confirmed versatility of sulfonated carbons prepared from *Mesua ferrea* L. seed DOWC [25]. Biomass from different sources have different properties which influence its reactivity during conversion processes (carbonization, activation, combustion etc.) the present work is an endeavor to understand the structure of DOWC biomass based sulfated carbon catalysts and to investigate effects of raw material properties and preparation methods on the structure, stability and activity of such catalysts using DOWC biomass obtained from three different sources as catalyst precursor (*J. curcas*, *P. pinnata* and *M. ferrea* L. seeds). Furthermore, to investigate feasibility of these biodiesel waste derived materials as catalysts in biorefining their catalytic performance were evaluated in two important reactions involved in biomass conversion, cellulose saccharification and fatty acid esterification (Schemes 1 and 2).

## 2. Experimental

### 2.1. Materials

*ortho*-Phosphoric acid (88%, Merck), oleic acid (Pure, Merck), sulfanilic acid (99%, Merck), $NaNO_2$ (98%, Merck), $H_3PO_2$ (30–32%, SRL) anhydrous $Na_2SO_4$ (99.5%, Merck), $H_2SO_4$ (98%, Merck), HCl (35%, Merck), acetone (99.5%, Merck), methanol (99.9%, Merck), ethanol (99.9%, Merck), 1-propanol (99.5%, Merck), 1-ethyl-3-methylimidazolium chloride (>99%, Merck), microcrystalline cellulose (Sigma) were purchased from commercial sources and used as received.

### 2.2. Catalyst preparation

The commercial zeolites H–Y [$SiO_2/Al_2O_3 = 12$, surface area = 884 $m^2/g$, acidity = 0.83 mmol$H^+/g$] and H-ZSM-5 [$SiO_2/Al_2O_3 = 23$, surface area = 443 $m^2/g$, acidity = 1.14 mmol$H^+/g$] were purchased from zeolyst International and calcined at 450 °C for 24 h prior to use. The precursors of carbon catalyst *J. curcas* (J), *P. pinnata* (P) and *M. ferrea* L. (M) seed DOWC, left after oil extraction by Soxhlet method were collected as wastes from Biofuel and Biomass conversion Laboratory, Tezpur University, Assam, India. Prior to carbonization/activation DOWCs were ground and sieved to make particles of size <250 μm (Chemical composition, Table 1). In this work three different approaches were adopted for the preparation of catalytic materials.

#### 2.2.1. Method 1 (4-benzenediazoniumsulfonate or radical sulfonation method)

To prepare the activated carbon (AC) supports (common step for methods 1 and 2), DOWC biomass pre-soaked with 50% (v/v) phosphoric acid were subjected to activation at 500 °C as described in our earlier work [24,25]. The activation temperature was fixed at 500 °C as materials obtained at this temperature exhibited maximum surface area and carbon content. Here, the final AC yields were recorded to be 36%, 35% and 20% on dry weight basis for M, P, and J de-oiled cakes, respectively, after washing and drying steps. Consequently, AC's were designated as MAC, PAC and JAC, respectively, where M, P and J represent the respective carbon precursor (raw materials). For comparison, biomass samples were also carbonized at 500 °C as control without using the activating agent. Prior to sulfonation the carbonized materials were powdered using a mortar and pestle and sieved through an ASTM no. 60 sieve to prepare particles with an average size of <250 μm.

**Table 1**
Composition of raw material (DOWC) before and after carbonisation.

| Properties | DOWC | | | Carbonsised/activated de-oiled cake | | | |
|---|---|---|---|---|---|---|---|
| | M | P | J | MAC | PAC | JAC | MACHT |
| Elemental analysis (wt%) | | | | | | | |
| C | 48.6 | 43.7 | 42.5 | 77.3 | 78.6 | 53.38 | 54.1 |
| H | 7.4 | 6.6 | 5.4 | 2.82 | 2.2 | 3.12 | 5.01 |
| N | 3.6 | 3.2 | 10.7 | 3.2 | 3.1 | 7.40 | 7.49 |
| O[a] | 40.3 | 46.5 | 41.4 | 16.7[b] | 16.1[b] | 34.2[b] | 27.95 |
| S | – | – | – | – | – | – | 5.45 |
| Biochemical analysis (wt%) | | | | | | | |
| Protein | 20.2 | 22.8 | 61 | – | – | – | – |
| Carbohydrate | 79.8 | 77.2 | 39 | – | – | – | – |
| Lipid | Trace | Trace | Trace | – | – | – | – |
| Proximate analysis (wt%) | | | | | | | |
| Moisture | 4.1 | 3.8 | 4.4 | 21.9 | 19.6 | 16.3 | 18.2 |
| Volatile matter | 82.6 | 80.1 | 74.1 | n.d. | n.d. | n.d. | n.d. |
| Fixed carbon | 8.4 | 11.9 | 16.6 | 11.9 | n.d. | n.d. | n.d. |
| Ash | 4.8 | 4.1 | 4.9 | 1.1 | 1.8 | 1.9 | <0.5 |

n.d. = not determined.
[a] Based on difference (ash free basis).
[b] (O + P) in phosphoric acid activated samples.

In this method, sulfonation was achieved via covalent attachment of aryl radicals generated by reduction of 4-BDS (4-benzenediazoniumsulfonate) in the presence of $H_3PO_2$ (Scheme 3) as described in our earlier work. Herein the method was applied with some minor modifications (increased amount of sulfonating agent) [25]. In a typical process, sulfanilic acid (15.2 g) was dispersed in 1 M HCl aqueous solution (300 mL) in a three necked flask. Then the flask was moved to an ice water bath, and the temperature was controlled at 3–5 °C with continuous stirring. Followed by an addition of 10% excess of 1 M $NaNO_2$ (90 mL, aqueous solution) dropwise, a clear solution was obtained after all the $NaNO_2$ was added. After stirring for another 1 h at the same temperature, the white precipitate of 4-BDS (~16 g) formed was filtered off, washed with deionized water and transferred to a 500 mL beaker containing deionized water (200 mL) and ethanol (60 mL). To this mixture, 1.5 g AC was added maintaining the temperature at 3–5 °C, followed by subsequent addition of 30–32% $H_3PO_2$ aqueous solution (100 mL). After stirring for 30 min, another 50 mL of $H_3PO_2$ was added and allowed to stand for another 1 h (or until $N_2$ evolution had ceased) with occasional stirring. The obtained sulfonated carbons were intensively washed with acetone and distilled water and then dried in the vacuum overnight and labeled as PACS (derived from P DOWC), MACS (derived from M DOWC), JACS (derived from J DOWC), respectively [25].

#### 2.2.2. Method 2 (direct $H_2SO_4$ sulfonation)

In this method, the sulfonated catalysts were prepared by direct sulfonation of DOWC based AC obtained above (using MAC as reference) with $H_2SO_4$ (98%) (Scheme 4) [12]. Briefly, 20 g $H_2SO_4$ (98%) was mixed with 1 g MAC and refluxed at 180 °C for 8 h. The obtained black products ($MAC_2SO_4$) were filtered, thoroughly washed with acetone, deionized water and then dried in vacuum overnight.

#### 2.2.3. Method 3 (hydrothermal $H_2SO_4$ sulfonation)

These carbons were prepared by one step hydrothermal treatment of DOWC (*M. ferrea* L. also used as a reference) with conc. $H_2SO_4$ (98%) as reported by Zhang et al. (Scheme 5) [26]. In a typical process, a mixture of 5 g DOWC and 25 g conc. $H_2SO_4$ (98%) were heated in a 200 mL Teflon-lined autoclave, at 180 °C for 24 h [26]. The obtained black products (MACHT) were filtered, thoroughly washed with acetone and deionized water and then dried in the vacuum overnight. Similar to the ACs all the sulfonated materials were powdered and sieved to particles size <200 μm prior to use.

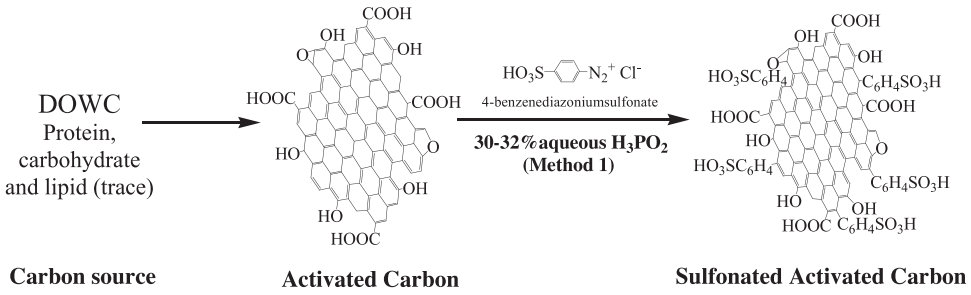


**Scheme 3.** Preparation of sulfonated carbons by functionalization of 4-BDS or radical route.

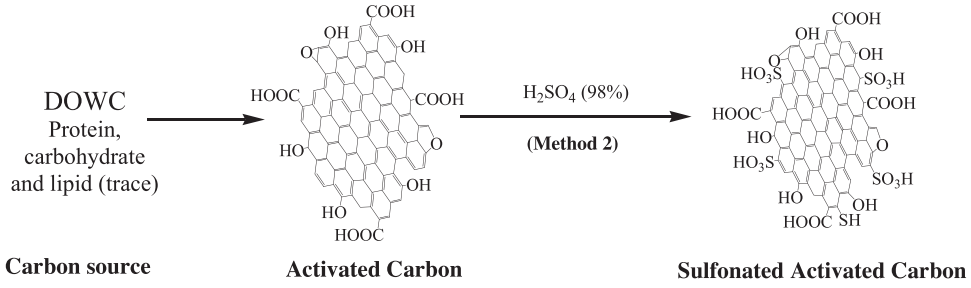


**Scheme 4.** Preparation of sulfonated carbons by $H_2SO_4$ or direct sulfonation route.

### 2.3. Catalyst characterization

The powder X-ray powder diffraction (XRD) patterns of carbon samples were recorded on a Rigaku miniflex diffractometer (Cu-Kα radiation, λ = 1.5406 Å) in 2θ range 10–70° at a scanning rate of 4 °C min$^{-1}$. FT-IR spectra were recorded in KBr pellets on a Nicolet (Impact 410) FT-IR spectrophotometer. Laser Raman micrographs were obtained on a Renishaw in Via laser Raman microscope using 514.5 nm laser. The elemental composition (bulk) of the carbonized materials and the carbon sources were determined by organic elemental analysis (OEA) on a Thermo Scientific FLASH 2000 apparatus. The oxidation state of surface functionalities, including the presence of —$SO_3H$ and phosphates groups were evaluated by X-ray photoelectron spectroscopy on a Kratos Axis Ultra DLD spectrometer with a monochromatized Al Kα X-ray source that was operated at 14 kV, 300 W. The analyzer pass energy was 17.9 eV and the energy step was 0.1 eV. The vacuum chamber base pressure was 10–9 mbar. The morphological features of the sulfonated carbons were studied by scanning electron microscopy (SEM) on a Zeiss Leo Gemini microscope operating at 20 kV. The elemental composition and the corresponding element mapping distributions were also obtained on a Jeol, JSM-6290LV instrument operating at 20 kV by energy-dispersive X-ray analysis (EDX). Transmission electron micrographs (TEM) were recorded on a Jeol JEM-2100 electron microscope operating at 200 kV. The resolution was around 0.4 nm. Samples were suspended in ethanol and deposited straight away on a copper grid prior to analysis.The specific surface area, pore size and pore volume of the carbon materials were determined by means of $N_2$ physisorption at liquid nitrogen temperatures on a Carlo Erba Sorptomatic 1990 instrument. The specific surface area was determined by the BET equation ($P/P_0$ = 0.05–0.3). The pore size distribution was determined from the desorption branch of the isotherm using the Barrett–Joyner–Halenda (BJH) method. The micropore volume was calculated via the Dubinin–Radushkevich method. The samples were pre-treated at 150 °C while degassing (∼0.1 Pa). The thermal stability of the catalytic materials were investigated by thermo gravimetric analysis (TGA-50, Shimadzu) from room-temperature to 500 °C at a ramping rate of 10 °C min$^{-1}$ under $N_2$ flow (UHP grade). The surface acidities were measured by temperature-programmed adsorption-desorption of ammonia on an AutoChem 2910, Micromeritics instrument. Briefly, 0.1 g sample was placed in an adsorption vessel (*U*-shaped) and activated at 150 °C in He flow for 2 h (heating rate 10 °C/min). Then the sample was cooled to 120 °C in He flow. At this temperature, 5% $NH_3$ in He was passed through the sample for 1 h followed by cooling to 100 °C in He flow. TPD was carried out from 100 to 500 °C at a heating rate of 10 °C/min with He flow rate of 35 mL/min. After each TPD measurements, the amount of ammonia adsorbed was

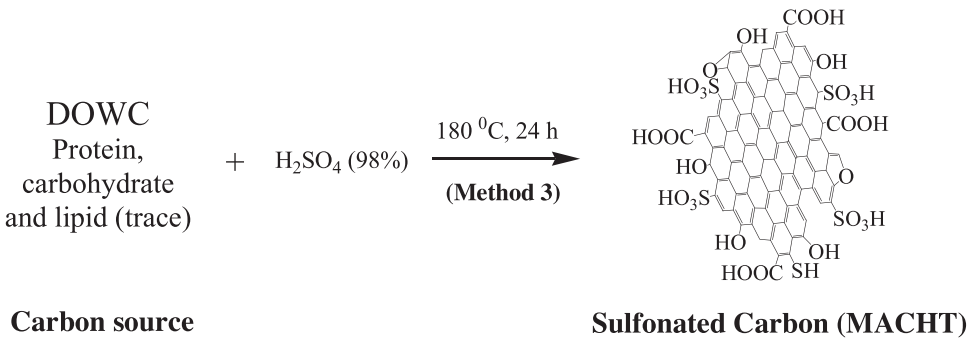


**Scheme 5.** Preparation of sulfonated carbons by one step hydrothermal route.

determined form the calibration curve obtained from varying volumes of ammonia in He. Further, the acid exchange capacities of the catalytic materials were determined by acid-base titration method as reported previously [25].

### 2.4. Evaluation of catalytic properties

#### 2.4.1. Cellulose hydrolysis

Reactions were performed in batch mode in 2 mL mini autoclaves (Supporting information) on a hot plate at temperatures of 100 °C, 120 °C and 150 °C, respectively, under autogenous pressure according to the conditions described by Onda et al. [27]. In brief, 0.01 g of cellulose, 0.01 g of catalyst (particle size <200 μm) and 1 mL distilled water were loaded into the autoclaves, heated to desired reaction temperature and held at this temperature for 24 h. After completed reaction, the mini-reactors were immediately cooled under tap water to quench the reaction. The reaction mixture were taken out and centrifuged to separate the solids (containing catalyst and the unreacted cellulose particles). Thereafter, the liquid phase was analyzed by means of high-performance liquid chromatography, (Hitachi HPLC LaChromUltra) equipped with Aminex HPX-87C column. The individual products were identified using commercially available standards and the yield was calculated from following the equation reported by Onda et al. [27]:

$$\text{Yield (mol} - \text{C\%)} = \frac{\text{mol of glucose/HMF} \times 6}{\text{mol of C in the cellulose (elemental analysis)}} \times 100 \quad \text{(iii)}$$

Conversions were based on the weight difference between unreacted cellulose and cellulose fed into the reactor and catalyst turnover frequency (TOF) was expressed as moles glucose formed per mole of acid site per hour. Here, the amorphous cellulose substrate was prepared by ionic liquid pretreatment as follows: In a typical process, 0.5 g microcrystalline cellulose was dissolved in 9.5 g 1-ethyl-3-methylimidazolium chloride ionic liquid and heated at 130 °C for 1.5 h with occasional stirring. Cellulose was regenerated by adding hot distilled water to the resulting solution, separated by filtration and dried at 100 °C.

#### 2.4.2. Oleic acid esterification

Esterification reactions were performed in a 100 mL three necked flask equipped with a magnetic stirring and a digital thermometer in an oil bath. Reactions were performed with oleic acid (the most common fatty acid found in vegetable oils) using 3 wt% catalyst loading at methanol reflux temperature with varying alcohol to acid molar ratios (5–30). In a typical reaction, 0.15 g catalyst (particle size <200 μm, outgassed at 150 °C) was added to appropriate amount of methanol/ethanol/2-propanol and heated to 64 °C and followed by an addition of 5 g preheated oleic acid with vigorous stirring (300 rpm) for 10 h. At selected time intervals, 0.1 mL aliquots were drawn from the reaction mixture centrifuged at 6000 rpm for 3 min to separate the catalyst particles. The acid value of the lower ester layer was determined by titration (in triplicates) after removal of excess methanol with standard KOH (0.01 mol $L^{-1}$) solution [25]. The conversion was calculated as:

$$C_{Est}(\%) = \frac{(C_i - C_t)}{C_i} \times 100 \quad \text{(i)}$$

where $C_i$ and $C_t$ are the acid value at 0 min and $t$ min, respectively. The ester formation and aromatic leaching was also verified by $^1$H NMR analysis of reaction mixtures following completion of reaction on a Jeol JNM-ECS400 NMR spectrometer at 25.5 °C using $CDCl_3$ as solvent and TMS as the internal standard [28]. The rate constant, '$k$' was calculated from the slope of time ($t$) vs. $\ln(1 - (C_{Est}/100))$ plots.

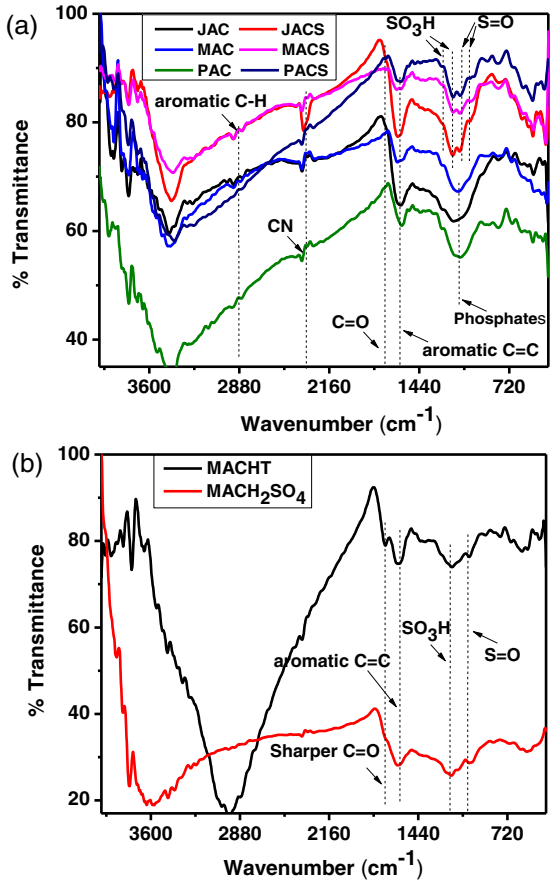


**Fig. 1.** FT-IR spectra of catalytic materials obtained from DOWC biomass: (a) prepared by method 1 (sulfonation with 4-BDS) with their non-sulfated forms (AC) and (b) prepared by conc. $H_2SO_4$ treatment (methods 2 and 3).

The TOFs were calculated using '$k$' values according to the equation below [20].

$$\text{TOF} = \frac{k \times C}{n_S} \quad \text{(ii)}$$

where $C$ denotes the amount of oleic acid (in mmol) loaded into the reactor and $n_s$ is the amount of strong acid (—$SO_3H$) sites on the catalyst loaded into the reactor.

## 3. Results and discussion

### 3.1. Catalyst structure and surface properties

#### 3.1.1. X-ray powder diffraction

The XRD patterns of the DOWC based sulfonated carbons clearly demonstrated the amorphous nature of these materials (Supporting information). All carbon samples exhibit a similar, broad and weak (0 0 2) diffraction peak near $2\theta = 15–30°$, with varying intensities corresponding to an amorphous carbon structure with randomly oriented polycyclic aromatic carbon sheets. The least intense and broad 0 0 2 peak recorded for hydrothermal sulfonated carbon (method 3) was indicative of its highly amorphous and functionalized structure resulting from partial carbonization, while prominent 002 peak for chemically activated sulfonated carbons was suggestive of a more order structure (methods 1 and 2). Further, in the XRD patterns of sulfonated carbons obtained from MAC and PAC, the additional (1 0 1) graphitic structure peak at $2\theta = 35–50°$ also appeared. The variations in XRD patterns and the properties of the resulting catalyst materials were strongly influenced by the choice of carbon precursor (biomass properties) and

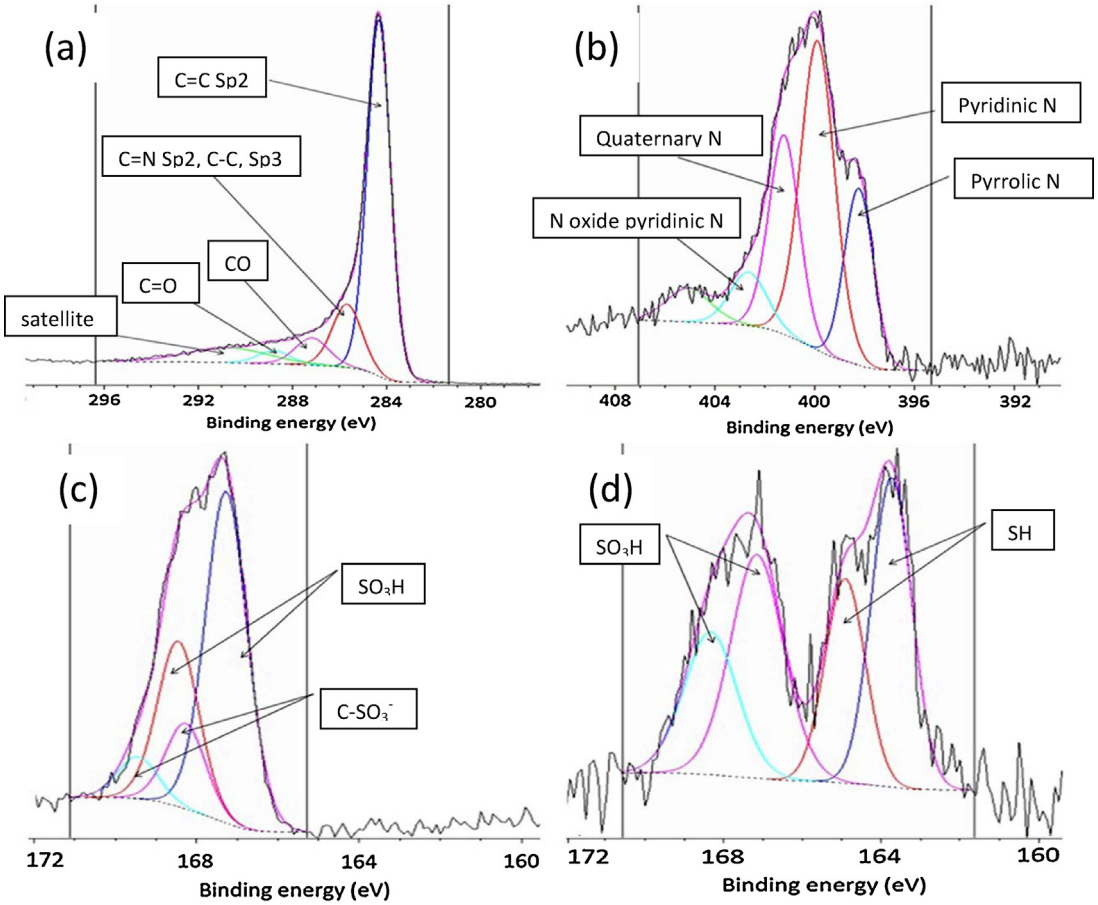


**Fig. 2.** High-resolution XPS spectra of a representative sulfonated carbon catalyst MACS showing the (a) C1s peak, (b) N1s peak (c) S2p peak and(d) S2p peak of $MACH_2SO_4$.

preparation method (more specifically the carbonization step, see Supporting information) [13,18–20]. The non-sulfonated materials (Figure not shown) also exhibited similar XRD patterns, in accordance with effect or raw material and further indicating that carbon samples did not undergo any morphological changes during the sulfonation process [25].

### 3.1.2. FT-IR spectroscopy

The FT-IR spectra of all carbons samples (Fig. 1) exhibited the typical bands of carbonyl groups (C—O, C═O, near 1700 $cm^{-1}$) and characteristic peaks of incompletely carbonised materials, near 1580 $cm^{-1}$ attributable (C═C) to aromatic ring modes with varied absorbance. The structural difference of these proteinaceous biomass derived materials from the typical carbohydrate or sugar based catalysts were apparent from the presence of the nitrile band near ~2360 $cm^{-1}$ and a broad phosphate band between 1300 and 900 $cm^{-1}$ due to incorporation of N and P into AC structures during carbonisation [29,30]. The sharper C═O bands for hydrothermally prepared MACHT and carbon samples obtained from J cake (JAC, JACS) in comparisons to those obtained by activation of M and P cakes were in accord with their functionalized surface structures. While, the increased C═O band intensity of $MACH_2SO_4$ as compared to MAC confirmed the formation of weak acid groups like —COOH along with —$SO_3H$ by oxidising effect of conc. $H_2SO_4$ on MAC surface and in good agreement with the trends found in literature (Fig. 1(b)), in contrast sulfonation by 4-BDS did not cause any such changes in C═O band intensity (Fig. 1(a)) [4,10,13]. Also, the success of sulfonation process and presence —$SO_3H$ and —$PhSO_3H$ groups on the surface of sulfonated carbons was confirmed by the emergence additional bands at 1110–1118 $cm^{-1}$ and 1003–1018 $cm^{-1}$ (S═O stretching), 1171–1175 $cm^{-1}$ and 1267–1270 $cm^{-1}$ (stretching in —$SO_3H$) in the FT-IR spectra of these materials [9,18,20,25].

### 3.1.3. Raman spectroscopy

Raman spectra of carbon samples exhibited the characteristic peaks of amorphous carbon at 1339 $cm^{-1}$ and 1600 $cm^{-1}$, corresponding to the defects induced D-band vibrations and the tangential C—C stretching G-band vibration due to integrity of hexagonal carbon (Supporting information). $I_D/I_G$, intensity ratio of D and G band is a measure of structural order and has been used as an tool to identify structural changes (e.g., disordering, clustering etc.) in carbon materials due to treatments such as annealing, oxidation and chemical functionalization [25,33]. Typically the ratio were in the order of ~0.64–0.86 for the chemically activated carbons while the same was >1 for the hydrothermally obtained or non-activated carbons, consistent with the more ordered graphitic structure of the former (Table 3). Further, as in our previous study upon sulfonation by method 1, the $I_D/I_G$ intensity ratio of ACs increased by 3–7% due to incorporation of additional —$PhSO_3H$ groups on the carbon frameworks which cause intensity of defects induced D vibrations to increase. Alternatively, the same changes were not observed for carbon materials sulfonated by method 2 (Table 3) presumably due to less effective —$SO_3H$ functionalization. Furthermore, based on these intensity ratios, the graphitic cluster sizes ($L_a$) in the carbon samples were also estimated using the Knight formula and presented in Table 3 [18,25,33].

### 3.1.4. X-ray photoelectron spectroscopy

XPS surface analysis further confirmed the structural differences of the DOWC biomass based catalysts from the typical

**Table 2**
Deconvolution of XPS peaks of the carbon materials obtained from DOWC.

| Peak | Assignment | JAC Position (eV) | JACS Position (eV) | PAC Position (eV) | PACS Position (eV) | MAC Position (eV) | MACS Position (eV) | MACH$_2$SO$_4$ Position (eV) |
|---|---|---|---|---|---|---|---|---|
| C1s | C=C, sp2 | 284.6 | 284.6 | 284.4 | 284.3 | 284.3 | 284.3 | 284.5 |
| | C=N sp2 and C=C sp3 | 285.7 | 285.8 | 285.6 | 286 | 285.5 | 285.7 | 286 |
| | C—O | 287.2 | 287.3 | – | – | 286.8 | 287.1 | 287.2 |
| | C=O | 288.4 | – | 287.1 | 287 | 288.1 | – | – |
| | COO | – | 288.8 | 288.2 | 288.1 | 289 | 288.8 | 288.9 |
| | Satellite | 289.7, 291.6 | 291.1 | 290.3 | 290.6 | 290.9 | 291 | 291 |
| O1s | =O in CO, COOH, PO, SO | 530.7 | 530.8 | 530.5 | 530.8 | 530.4 | 530.9 | 530.7 |
| | —O— | 532.8 | 532.5 | 532.4 | 532.5 | 532 | 532.6 | 532.1 |
| | Chemisorbed O + $H_2O$ | 536 | 534.5 | 536.8 | 534.6 | 533.5 | – | 533.3 |
| N1s | Pyridinic N | 398.4 | 398.3 | 398.2 | 398.1 | 398.3 | 398.2 | 398.2 |
| | Pyrrolic N | 400 | 400 | 399.9 | 399.8 | 399.8 | 399.9 | 400.1 |
| | Quaternary N | 401.2 | 401.8 | 401.2 | 401.3 | 400.9 | 401.3 | 401.5 |
| | N oxide of pyridine N | 403.1 | – | 403.1 | 403 | 404.2 | 402.6 | 403.3 |
| P2p | $PO_4$ | 133.4 | 134.5 | 133.4 | 133.5 | 133.4 | 133.4 | 133.4 |
| S2p | —SH | – | – | – | – | – | – | 163.8 |
| | C—$SO_3^-$ | – | 167.2 | – | 167.2 | – | 167.3 | – |
| | $SO_4^{2-}$ or —$SO_3$H | – | 168.1 | – | 168.3 | – | 168.3 | 167.1 |

carbohydrate, sugar and resin based catalysts. The XPS spectra of these materials revealed a more complicated surface structure which resembled N-doped carbons rather than the AC, in addition to the C, O, S typically reported in sulfonated carbons (Supporting information) they also contain several N and P species (in phosphoric acid activated samples) [4,11,13]. The deconvolution of high-resolution of C1s, N1s and O1s regions confirmed the presence of several carbon species (Fig. 2 and Table 2). Here, the C1s region was resolved into five components (Fig. 2(a)); the main peak at 284.4 ± 1 eV was assigned to sp2-hybridized graphite-like carbon (C=C sp2), the peak at 285.7 ± 2 eV was assigned to the overlapping signal of C=N sp2 carbon and C—C sp3 carbon, while the small peaks centered at 286.8–287.2, 287.8–288.1 and 288.2–288.8 eV were attributed to C—O, C=O and —COO corresponding to the various surface functional groups [31]. Also, the more prominent C1s sp2 region in the chemically activated MAC and PAC was consistent with their more aromatized carbon structures. The N1s region (Fig. 2(b)) was similar to the N-doped carbons and deconvoluted into four main components; the lowest binding energy peak at 398.1–398.3 eV originated from the presence of pyridinic N, while the peaks at 399.3 eV, 401 eV and 402.4 eV were ascribed to pyrrolic, quaternary and N-oxide of pyridinic N, respectively. The higher percentage of N species in Jatropha caked derived materials could attributed to its higher protein content (~11% N) which upon activation carbonised into carbon nitride like films (Supporting information, Table 1) [32]. The O1s region was also resolved into three main components (Supporting information). The single P2p peak at 133.5 ± 1 eV in the phosphoric acid activated carbons also suggested the existence of pentavalent tetracoordinated phosphate compounds ($PO_4$ or polyphosphates) in their structure (Table 2) [31].

Generally, the S2p photoelectron peak (163–168 eV) is of particular significance in the sulfonated materials and has been used to confirm the presence of —$SO_3$H groups [4–20]. Here, XPS surface analysis also revealed the effects of preparation method on catalyst surface structure. In this work, the AC sulfonated by radical method (method 1) exhibited only a single S peak at 168 eV, assigned to the surface bound —$SO_3$H groups, while those prepared by conc. $H_2SO_4$ treatment (methods 2 and 3) exhibited an additional thiolate peak near 163 eV. The presence thiolate peak was also reported by Shu et al. [13] for an oil pitch derived catalyst obtained by $H_2SO_4$ sulfonation, but interestingly authors assumed all S to be —$SO_3$H. A possible explanation for the presence of —SH groups could be related to the oxidation of the some of the —OH/—H groups on AC surface to —COOH at the expense of the oxidising effects neighboring —$SO_3$H groups at high sulfonation temperatures (180 °C). We

**Table 3**
Surface and textural characteristics of the carbon materials obtained from DOWC.

| Catalyst | [a]$S_{BET}$ m$^2$/g | [b]$V_p$ cm$^3$/g | [c]$D_p$ nm | [d]$V_{mp}$ cm$^3$/g | $I_D/I_G$ | [e]$L_a$ nm | [f]—$SO_3$H density mmol/g | [g]Total acid density mmolH$^+$/g | [h]$NH_3$ acidity mmol/g | [i]$T_{max}$ °C |
|---|---|---|---|---|---|---|---|---|---|---|
| JAC | 423 | 0.32 | 3.93 | 0.15 | 0.79 | 5.56 | – | 3.24 | 4.34 | 470 |
| PAC | 914 | 0.77 | 6.7 | 0.35 | 0.64 | 6.72 | – | 2.58 | 2.01 | 500 |
| MAC | 786 | 0.63 | 4.4 | 0.28 | 0.86 | 5.07 | – | 1.91 | 1.76 | 500 |
| JACS | 93 | 0.23 | 3.9 | 0.13 | 0.86 | 4.9 | 0.70 | 3.96 | 6.20 | 240 |
| PACS | 483 | 0.46 | 4.8 | 0.17 | 0.66 | 6.68 | 0.84 (0.83) | 3.62 | 5.86 | 248 |
| MACS | 468 | 0.39 | 4 | 0.17 | 0.90 | 4.85 | 0.75 | 3.01 | 5.63 | 245 |
| MACH$_2$SO$_4$ | 690 | 0.61 | 4.1 | 0.26 | 0.86 | 5.07 | 0.30[j] (0.13) | 2.01 | n.d. | n.d. |
| MAC-$SO_3$H [25] | 556 | n.r. | 4.9 | 0.19 | n.r. | 4.89 | 0.73 | 2.426 | – | 242 |
| MACHT | <1 | – | – | – | 1.1 | n.d. | 1.30[j] | 4.2 | 6.4 | n.d. |

n.d. = not determined, n.r. = not reported, MAC-$SO_3$H [25] prepared by method 1 from MAC but with a lower 4-BDS:MAC w/w ratio of 2:1.
[a] Specific surface area.
[b] Total pore volume at $P/P_0$ = 0.95.
[c] Average pore diameter.
[d] Micropore volume.
[e] $L_a = C_\lambda/(I_D/I_G)$, where $C_\lambda$ = 4.4 nm.
[f] Based on elemental analysis (represent values for spent catalyst after 3rd esterification cycle).
[g] Based on titration.
[h] Based on $NH_3$-TPD measurements.
[i] Based on TGA in $N_2$.
[j] = (—$SO_3$H + —SH).

observed similar —SH peaks when the —$SO_3H$ containing materials were reduced by strong reducing agents (e.g., $H_3PO_2$). The possibility of elemental sulfur was ruled out as the non-sulfonated (AC) materials did not exhibit any S peaks. This observation further strengthened the advantages of 4-BDS over conc. $H_2SO_4$ as a sulfonating agent. The non-sulfonated carbon materials also exhibited similar XPS patterns, only difference being the absence of S2p peak (Supporting information). Overall, due to the unique composition of raw material (DOWC biomass), the sulfonated carbons reported herein are structurally more complex and contain pyridine like N groups (and also phosphates if activated by phosphoric acid) incorporated into their carbon framework, in addition to the —OH, —COOH and —$SO_3H$ groups found in carbohydrate, sugar and resin based sulfated carbons, respectively [4,11,13]. The raw material composition (i.e., protein vs. carbohydrate content) had direct effect on active carbon yield, chemical composition, textural and surface properties (see below). Under identical conditions, the yield, carbon content and structural order of AC:s decreased with increasing protein content (i.e., N%) in biomass. Thus, the percentage of N increased with increasing protein content of biomass.

### 3.1.5. $N_2$ physisorption and surface properties

The effects of biomass composition and preparation method on catalyst properties were also seen in the surface and textural properties of the various DOWC derived carbon catalysts (Table 3). The hysteresis in the isotherms of chemically activated materials was indicative of the presence of mesopores. Overall, the chemically activated sulfonated carbons (MACS, PACS, JACS and $MACH_2SO_4$, respectively) were found to be a mixture of mesoporous and microporous particles with high specific surface areas (93–690 $m^2/g_{cat}$), while the hydrothermally obtained catalyst (MACHT) was nonporous and exhibited low specific surface area (<1 $m^2/g_{cat}$) similar to the un-activated carbons (1–10 $m^2/g$, control samples, data not shown). Under identical conditions, the porosity development was only affected by the properties of the raw material. Here, PACS and MACS biomass (low protein or N%) derived AC:s and their sulfonated counterparts exhibited much larger specific surface area, pore diameter and higher mesopore contents than the JACS cake based materials (Table 3 and Fig. 3). Thus, the development of pores and proper carbonization were retarder when the raw material contained high amounts of protein. Successful sulfonation also gave rise to reduced pore size, pore volume and specific surface area of the sulfonated materials (Table 3). In this work, sulfonation of ACs by 4-BDS (method 1) resulted in pore volume reduction in the order of 28–40%, in pore diameters of 0.4–1.9 nm and specific surface areas of 300–400 $m^2/g_{cat}$. Consequently, this was consistent with the successful attachment of abundant bulky —$PhSO_3H$ groups, whereas such drastic changes were not observed in samples sulfonated by method 2, indicating less successful —$SO_3H$ incorporation. The differences could partly be attributed to the smaller size of —$SO_3H$ groups (Table 3 & Fig. 3) [7,20,34,35]. Further, as shown in Fig. 3(b), it was apparent that the sulfonation process occurred equally well in both meso and micropores, irrespective of the method applied.

### 3.1.6. —$SO_3H$ density

The catalytic effects of sulfonated carbon materials has been credited to —$SO_3H$ groups, thus its density has a distinct effect on catalyst activity [5]. The presence of S and increased surface acid site densities of the sulfonated DOWC derived materials were consistent with the success of sulfonation step (Table 3). The variations in —$SO_3H$ density (MACHT > PACS > MACS > JACS > MAC-$SO_3H$ > $MACH_2SO_4$) among these materials was in agreement with effects of raw material and preparation method on catalyst acidity. Comparison of the above trend and AC support properties in Table 1 revealed a clear relation between —$SO_3H$ density and

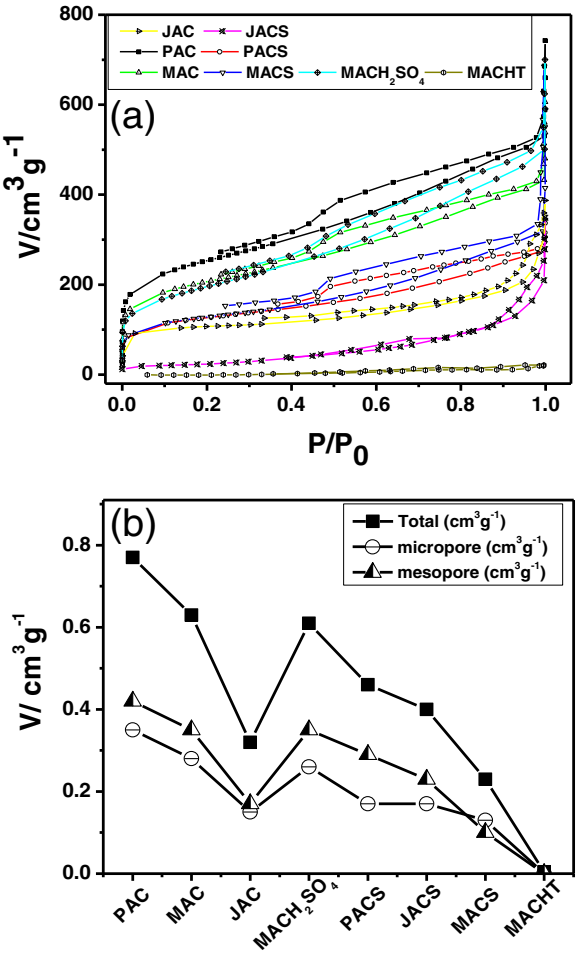


**Fig. 3.** (a) $N_2$ adsorption–desorption isotherms of carbon materials and (b) the corresponding pore volumes.

C contents of AC prepared by method 1. The increased —$SO_3H$ density with increasing C content in AC could be credited to the functionalization of additional 4-BDS radicals resulting from availability of more aromatic carbon sheets (Sp2 sites, evidenced by XPS, Tables 1 and 3) for —$PhSO_3H$ attachment. On the contrary the $H_2SO_4$ treated carbon, $MACH_2SO_4$ exhibited relatively low —$SO_3H$ density as it was difficult for $H_2SO_4$ to react with the rigid, aromatized and ordered frameworks of AC even at elevated temperatures [4,5]. Similarly, the high —$SO_3H$ density in MACHT (method 3) could be credited from the easier sulfonation of the partially carbonized (less aromatic) structures formed under hydrothermal conditions and consistent with literature data which suggests that non-graphitic carbons (less aromatized ones) are easier to react with $H_2SO_4$ than aromatized graphitic carbons [5,26]. Nonetheless, successful sulfonation of ordered carbon materials have been demonstrated with stronger sulfonating agents like fuming $H_2SO_4$, gaseous $SO_3$, $ClH_3SO_4/H_2SO_4$ mixture (which comes with their share of drawbacks such as handling issues, high energy requirement, accidental $SO_x$ release etc.) [4,11,34]. Consequently, the present study shows sulfonation by 4-BDS to be a more effective method for sulfonating carbon materials with aromatized or graphitic structure, contrary to the conventional sulfonation process (conc. $H_2SO_4$, $SO_3$) reported as a more efficient strategy for non-graphitic carbons [4,5,8,11–13]. Accordingly, the combination of activation (chemical or physical) and radical sulfonation (method 1) may be a valuable technique for obtaining sulfonated carbon catalysts from biomass which possesses high porosity and acidity simultaneously. Using the combination of above steps we have

been able to prepare mesoporous sulfonated carbon catalysts with pore volume ~0.46 $cm^3\ g^{-1}$, average pore diameter ~4.8 nm and $-SO_3H$ density upto ~0.84 mmol/g. Furthermore, the study also showed that the amount of 4-BDS/sulfanilic acid had negligible effect on catalyst $-SO_3H$ density as the M DOWC based catalysts MACS (prepared at 15:1 w/w ratio of sulfonating agent to AC) and MAC-$SO_3H$ (prepared by same method but with 4-BDS to AC w/w ratio of 2:1) exhibited comparable $-SO_3H$ densities (Table 3). Instead, this depends on the amount of Sp2C sites available (i.e., carbon content) for 4-BDS radical attachment [25]. In terms of weak acid sites, the sulfonated and non-sulfonated material exhibited similar —OH, —COOH density as sulfonation process (in particular method 1) did not affect the weakly acidic groups. Although, sulfonation with $H_2SO_4$ (98%) caused oxidation of some of the AC sheets its effect on overall material acidity was insignificant (Table 3).

### 3.1.7. TGA analysis

The reported catalysts showed excellent thermal stability under oxygen-free conditions which is comparable to the previously reported sulfonated carbon catalysts (Table 3). Overall, all the DOWC based catalytic materials demonstrated good operational stability and were suitable for applications at operating temperatures close to 240 °C. Based on results of TGA the catalysts prepared from P and M DOWC were found to exhibit 2–3% better stability than the *Jatropha* based catalyst due to their more ordered structures (higher aromaticity) and presence of lower amounts of surface functional groups (Table 3 and Supporting information). Fig. 4 shows the typical TGA patterns of the sulfonated carbons, which show two distinctive weight loss regions. The first, more rapid loss occurred between 0 and 130 °C, which was attributed to loss of water and free moisture adsorbed on the catalyst surface. The second weight loss region occurred at 240–380 °C; 6–8% weight loss in this region was attributed to the removal of $-SO_3H$ groups, as this region was absent in the non-sulfonated materials. Following the 2nd region, weight loss continued but at a much slower rate which could be credited to the graphitization of AC (Fig. 4). In short sulfonation lowered the onset of thermal decomposition due to incorporation of $-SO_3H$ groups on carbon surface. However, for JACS, the weight loss continued at the same rate even after 400 °C (2nd region). This could be attributed to further carbonisation of the material which occurred at elevated temperatures due to its functionalized structure [34].

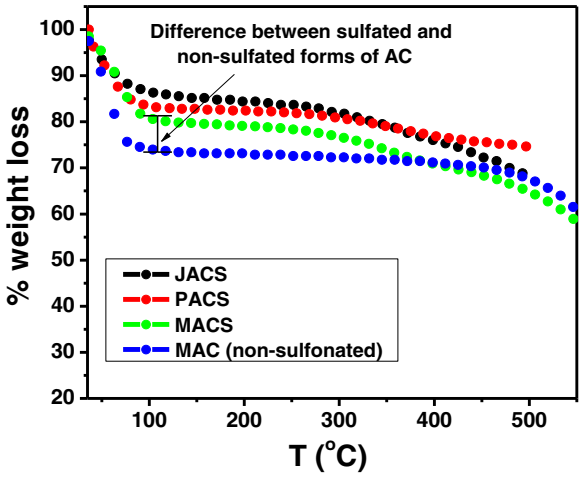


**Fig. 4.** Representative TGA patterns of the sulfonated carbon obtained from three different DOWC, the non-sulfonated material is shown as control.

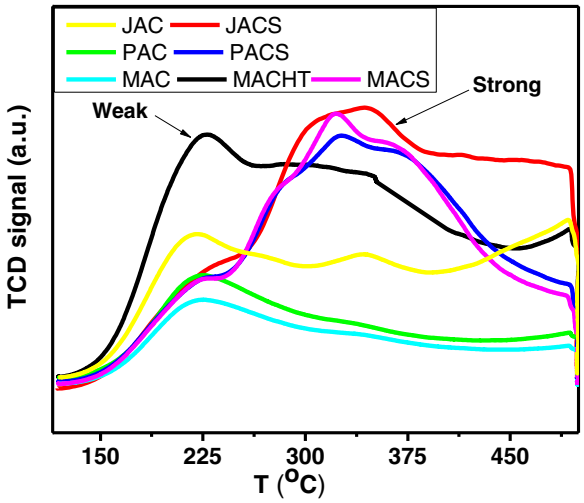


**Fig. 5.** Typical $NH_3$-TPD profiles of catalytic materials obtained from DOCW.

### 3.1.8. Temperature programmed desorption of ammonia

Fig. 5 shows the typical $NH_3$-TPD profiles of DOWC derived sulfonated carbons in comparison to the parent non-sulfonated forms. The $NH_3$ acidity calculated from TPD measurements are presented in comparison to the titration values in Table 3. The trend based on $NH_3$-acidty was in close agreement with acid exchange capacities (higher acidity for more functionalized materials) based on titration. In our experiments, we have restricted the TPD desorption temperature to 500 °C as sulfonation also reduces the thermal stability of carbonized materials and 500 °C was found to be the maximum temperature upto which most of the $-SO_3H$ remained attached to the catalyst surface, as also stated by Kastner et al. [34]. In all cases, we observed two distinctive peaks, a weak acid site around 210–230 °C and strong acid site 310–370 °C (Fig. 5). Here, the strong acid sites were ascribed to $-SO_3H$ and phosphate groups, whereas weak acid sites were attributed to the surface functional groups (—OH, —COOH and lactones) [34]. Further, the stronger weak acid peak in MACHT and JAC was in accord with their functionalized structures whereas the small peak at 310–370 °C in the non-sulfated materials (AC) was accounted by the presence of phosphates (Table 1). It is also worth pointing that $NH_3$-acidities based on TPD were approximately ~30% higher than the acid exchange capacities obtained by titration method, in good agreement with trends found in literature [14,34]. This overestimation can most likely be accounted for by desorption of SO*x* species along with $NH_3$ at temperatures 240–500 °C, due to removal of the sulfonic groups from catalyst surface; this, in turn, indicates the limitations of $NH_3$-TPD method for acidity measurements of sulfonated carbon materials. Nonetheless, it is interesting to note that many authors have used $NH_3$ desorption temperatures up to 750–800 °C for acidity measurements of similar materials without taking into account the stability of sulfonic groups whereupon erroneous estimation of acidity might occur [11,13]. Hence, the usefulness of $NH_3$-TPD method for acidity measurements of sulfonic acid functionalized materials should be reviewed.

### 3.1.9. Scanning electron microscopy and energy dispersive X-ray microelement mapping

SEM pictures clearly show that the morphology of the DOWC derived carbon materials were directly affected by the preparation method and carbon source, a clear difference existed in the topography of the chemically activated and the non-activated materials. The non-activated carbons clearly exhibited a non-porous topography while appearance of large cracks and holes was consistent

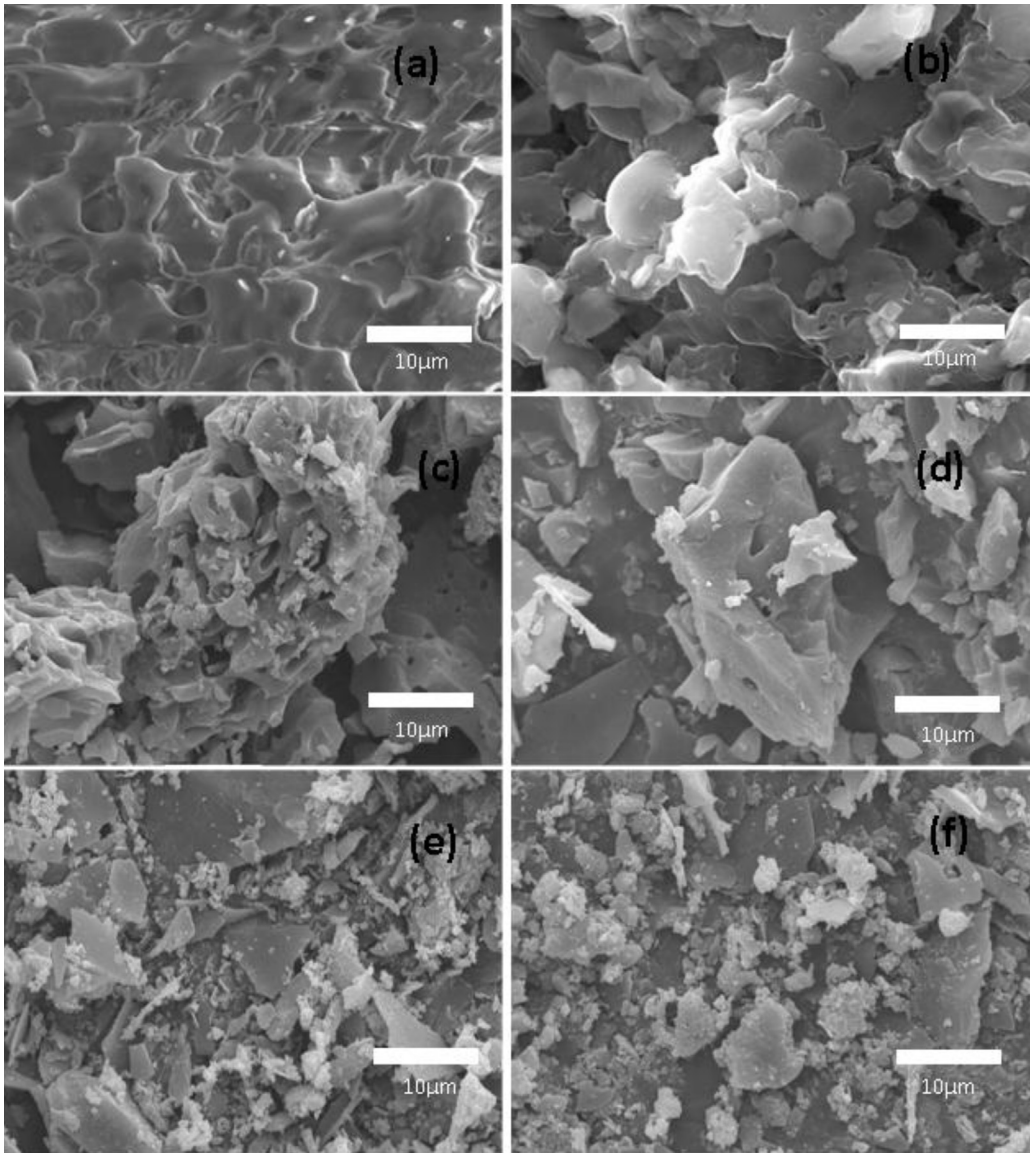


**Fig. 6.** SEM images of the carbon materials (a) MACHT (b) MAC* (unactivated) (c) MAC (d) MACS (e) JAC (f) JACS obtained from DOWC biomass under different conditions (scale 10 μm).

with development of meso and micro pores in the phosphoric acid treated materials (Fig. 6(a)–(c)). On the other hand, the effect of carbon source on porosity development could be clearly seen from the difference in topography of chemically activated J (flake like) and M (particle like) cakes (Fig. 6(c)–(f)). This effect was also seen in the SEM images of sulfonated catalysts obtained from the three different biomass sources under identical conditions (method 1) showing the presence of non-uniform and irregular particles of different size and shapes (Supporting information) [25]. SEM images also confirm that the carbon materials didnot undergo any morphological changes due to sulfonation (Fig. 6(c)–(f)). Also, the corresponding EDX element mapping (C, O and S) of these materials clearly indicated the homogenous distribution of the different surface acid sites (—$PhSO_3H$, —OH and —COOH) with no non-single element clusters. A comparatively high S density observed for PACS and MACS compared to JACS was in good agreement with the respective trend of —$PhSO_3H$ densities. On the other hand, the density of O (the weakly acidic or O containing sites) followed just the opposite order JACS > PACS ≥ MACS, consistent with their respective surface functional group densities (Supporting information).

### 3.1.10. *Transmission electron microscopy*

TEM micrographs (Fig. 7) of the catalysts MACHT, MACS, PACS and JACS clearly show the presence of a non-uniform carbon structure with randomly arranged aromatic carbon sheets in all the materials. The morphology was distinctly different for the hydrothermal MACHT and the chemically activated sulfonated carbons MACS, PACS and JACS. The non-activated catalyst, MACHT closely resembled the corncob derived sulfonated carbons reported by Arancon et al. [15]. While, the highly textured surface morphology and appearance of well developed mesopores in the chemically activated sulfonated carbons were in good agreement with the results of $N_2$ physisorption (Table 3). The effect of raw material on porosity development was further clarified from the dissimilar morphology observed for MACS, PACS and JACS; a highly textured and coarse surface morphology with well developed pores as large as ~11 nm observed for PACS and MACS were characteristics of a

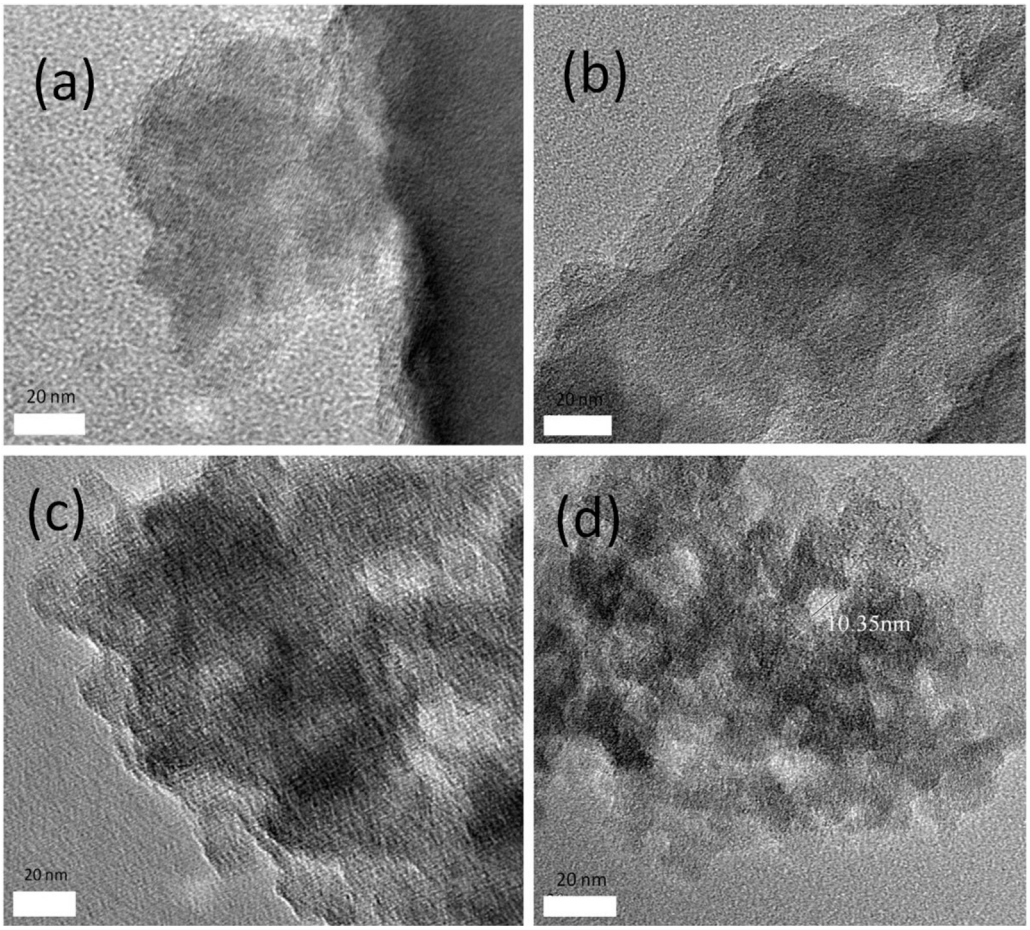


**Fig. 7.** HR-TEM images of the sulfonated carbons: (a) MACHT (b) JACS (c) MACS and (d) PACS (scale 20 nm).

dominant mesoporous structure and well reflected by their textural properties (Table 3), whereas JACS with its slightly less coarse morphology exhibited features typical to less porous material (Fig. 7) [15].

#### 3.1.11. Proposed structure of the DOWC derived catalytic materials

The above characterization results point to a much complex structure for the DOWC biomass derived sulfonated catalysts which different from the typical carbohydrate or sugar derived sulfonated carbons/sulfonated active carbons prepared by Hara et al. method [4]. Structurally these multifunctional materials are related more to the N-doped carbons or carbon nitrides rather than amorphous or active carbons [4]. In contrast to the typical carbohydrate or resin based sulfonated catalyst where the basic structural unit is simply a flexible aromatic carbon or graphene sheet functionalized with –OH, —COOH and —$SO_3H$ groups (I). The structural unit of sulfonated carbons obtained from the protein rich DOWC resembles a flexible carbon nitride sheet which has been extensively functionalized with —OH, —COOH, phosphates ($PO_4$) and —$SO_3H$ or —$PhSO_3H$ groups. The DOWC based catalytic materials may adopt any one of the three the structures II or III or IV depending on the method of preparation (Fig. 8). The density and nature of surface acidic groups are directly affected by carbonisation conditions (temperature, use of activating agent etc.). Here, the $H_2SO_4$ treated and phosphoric acid activated DOWC (method 2) will take up structure II while the materials prepared by method 1 (4-BDS treated) will adopt structure III and the hydrothermally sulfonated and carbonised materials (method 3) will take up structure IV.

### 3.2. Catalytic activity

#### 3.2.1. Cellulose hydrolysis

Hydrolysis of cellulose involves breaking of β-1,4-glycosidic bonds of the large polysaccharide units with $H_2O$ to produce the building monosaccharide. Saccharification or hydrolysis of cellulosic materials is an important step of biorefining which produce sugars; a valuable precursor in the production of bio-alcohols, biofuels and various fine chemicals [35]. It has been reported that over sulfonated materials hydrolysis takes place in two steps, the first step involving the breakdown of large polysaccharide units to water soluble oligomers (glucans), which are subsequently adsorbed on catalyst surface and hydrolyzed to sugars by the catalytic action of strongly acidic —$SO_3H$ groups/sites. Further, the weakly acidic —OH, —COOH groups/sites present in sulfonated carbon materials are reported to promote adsorption of these oligomers, thus density of such groups can greatly influence the catalytic efficiency of sulfonated materials in cellulose saccharification [4,5,36,37]. The results obtained for the DOWC based materials are in good agreement with the above effects. Data summarized in Table 4 clearly show the catalytic effects of DOWC based sulfonated materials compared to their non-sulfonated counterparts showing activity comparable to the blank reaction. Here, the negligible activities of un-sulfonated materials (ACs) are in agreement with non-catalytic effects of the weakly acidic (—COOH, —OH) [36,37] and the phosphate groups. In terms of molar glucose (sugar) yield, the sulfonated materials reported here, not only outperformed $H_2SO_4$ (0.1 mol/L), zeolites, ion-exchange resins and sulfated zirconia; in addition, some of these catalysts also outperformed a

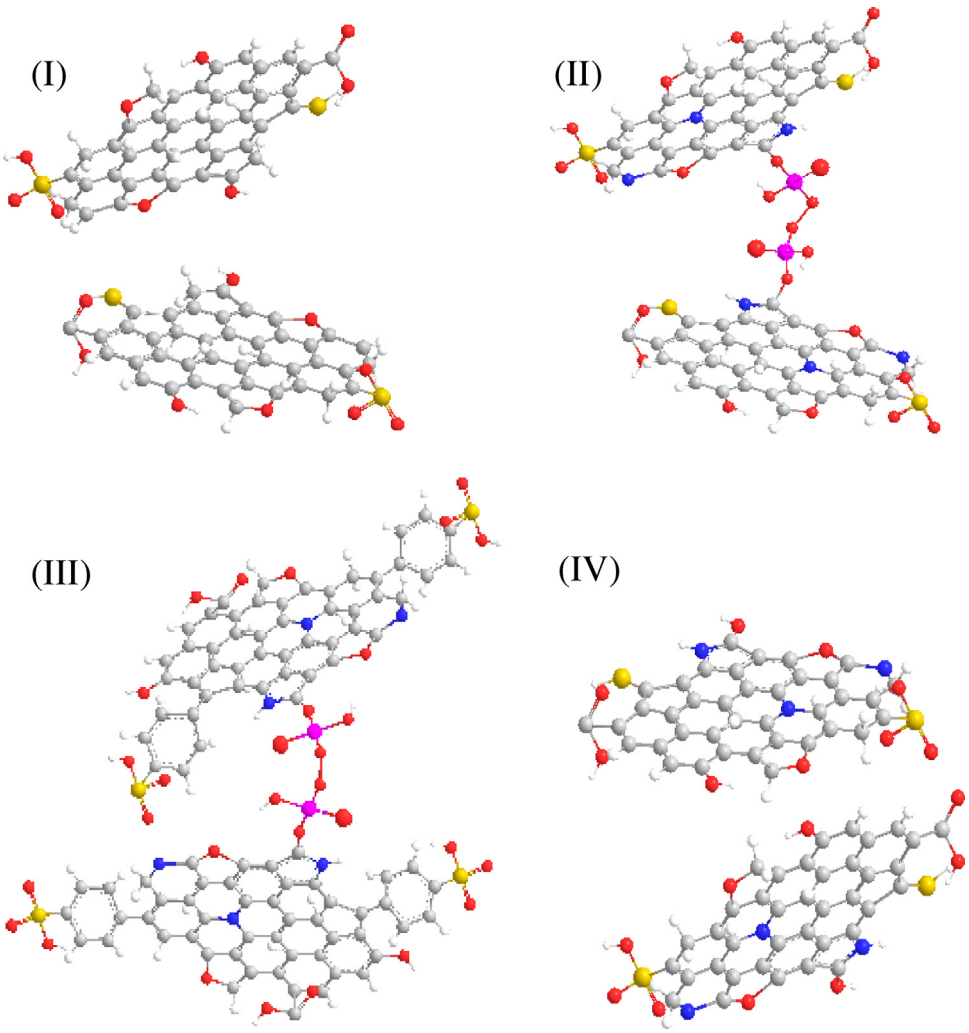


**Fig. 8.** Plausible structure for the structural units of (I) the typical carbohydrate or sugar or resin based sulfonated carbons, based on Hara et al. [4] method and the sulfonated carbon catalyst prepared from DOWC biomass by (II) method 2, (III) method 1 and (IV) method 3. Where, represent C, N, O, S, P and H, respectively. (For interpretation of the references to colour in this figure legend, the reader is referred to the web version of this article.)

number of sulfonated catalysts reported in earlier works (Table 4) [4,36–39]. As in the studies before, the sugar yields were influenced mainly by $-SO_3H$ density, porosity (pore size, surface area) and the density of weakly acidic sites on catalyst surface (in other words $mmolH^+/g_{cat}$) (Table 4). Among the reported catalysts, those obtained by method 1 (MACS, PACS and JACS), produced highest sugar yield (35–53 mol–C%) from amorphous cellulose in 24 h. In contrast, the materials obtained by $H_2SO_4$ treatment, MACHT and $MACH_2SO_4$ were relatively less active due their limited pore space and low $-SO_3H$ (strong acid site) density, respectively (Table 4). The

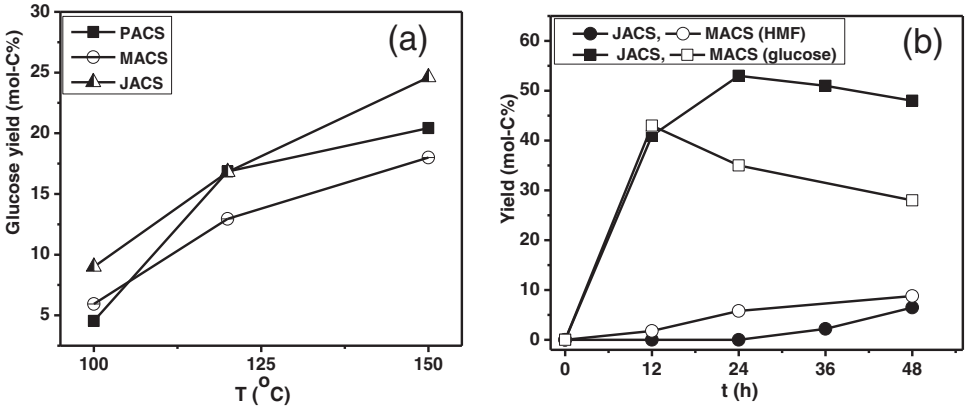


**Fig. 9.** Saccharification activity of the optimum DOWC biomass derived sulfonated carbon catalyst as function of (a) reaction temperature (investigated with microcrystalline or untreated cellulose substrate) and (b) reaction time (investigated with amorphous cellulose at 150 °C).

**Table 4**
Sacchrification activity of DOWC biomass derived catalyts.

| Catalyst | $S_{BET}$ $m^2/g$ | $D_p$ nm | $V_p$ $cm^3/g$ | —$SO_3H$ density mmol/g | Conversion % | Yield mol-C% | [a]TOF $h^{-1}$ | Refs. |
|---|---|---|---|---|---|---|---|---|
| Blank | – | – | – | – | 10 | 0 | 0 | This work |
| JAC | 423 | 3.93 | 0.32 | – | 10 | 8 | 0.0064 | |
| PAC | 914 | 6.7 | 0.77 | – | 10 | 6.6 | 0.0066 | |
| MAC | 786 | 4.4 | 0.63 | – | 10 | 6 | 0.0080 | |
| JACS | 93 | 3.9 | 0.23 | 0.70 | 61 | 53 | 0.0344 | |
| PACS | 483 | 4.8 | 0.46 | 0.84 | 60 | 46 | 0.0335 | |
| MACS | 468 | 4 | 0.39 | 0.75 | 60 | 35 | 0.0301 | |
| MACHT | <1 | – | – | 1.30 | 43 | 27 | 0.0164 | |
| $MACH_2SO_4$ | 690 | 4.1 | 0.61 | 0.19 | 52 | 30 | 0.0388 | |
| $H_2SO_4$ (0.1 mol/L) | – | – | – | – | 63 | 32 | 0.0079 | |
| H-Y (12) | 884 | – | – | 0.83[b] | 21 | 10 | 0.0316 | |
| JACS | 93 | 3.9 | 0.23 | 0.70 | 90[c] | 78[c] | 0.0503 | |
| $H_2SO_4$ (0.1 mol/L) | – | – | – | – | 61.8 | 32.7 | – | [27] |
| AC-$SO_3H$ | 806 | – | – | 0.44 | 42.8 | 40.5 | – | [27] |
| H-Beta (13) | 105 | – | – | 1.05[b] | 22 | 5 | – | [27] |
| H-ZSM (45) | 124 | – | – | 0.30[b] | 10 | 8 | – | [27] |
| Sulfated $ZrO_2$ | 52 | – | – | 1.20 | 38 | 18 | – | [27] |
| Amberlyst-15 | n.r. | – | – | 1.70 | 33.7 | 25.5 | – | [27] |
| CMK-3-$SO_3H$ | 412 | – | – | 0.63 | 95 | 74.5 | – | [36] |
| Resin carbon-$SO_3H$ | 834 | – | – | 0.28 | 62 | 54 | – | [36] |
| CSAC-$SO_3H$ | 981 | – | – | 0.33 | 60 | 45 | – | [36] |
| Cell-carbon-$SO_3H$ | 6 | – | – | 2.01 | 45 | 35 | – | [36] |
| MWCNT-$SO_3H$ | 92 | – | – | 0.02 | 50 | 27 | – | [36] |
| Si33C66-823-$SO_3H$ | – | – | – | 0.57[b] | 60.7 | 50.4 | 0.15 | [38] |

Reaction conditions: cellulose:catalyst (w/w ratio) = 1 (this work) and 0.9–1 for [27,36,38], 1 mL $H_2O$ per 0.01 g amorphous cellulose or [c]IL trated biomass (*Mesua ferrea* L. DOWC), $t$ = 24 h, $T$ = 150 °C.

[a] TOF = moles glucose formed per mole of acid site per hour.

[b] Total acidity ($mmolH^+/g_{cat}$).

[c] Yield = (6 × mol of glucose + 5 × mol of xylose)/mol of C in carbohydrate part of DOWC.

superior activity of the former are therefore attributed to the presence of larger pores, high surface area and suitable combination of the density of strong (0.70–0.84 $mmol/g_{cat}$) and weak surface (3.24–1.91 $mmolH^+/g_{cat}$) acid sites. Further, when microcrystalline cellulose was used as substrate sugar yield reduced by half (Fig. 9), which may be attributed to the difficulties associated with getting past the highly packed and crystalline structure of untreated cellulose (crystallinity index ~82%) [40]. Typically, previous studies have employed amorphous cellulose obtained by ball-milling (48–72 h) as substrate which are much easier to hydrolyze [4,36–40]. In contrast, here we have applied a more practical ionic liquid (IL) pretreatment with 1-ethyl-3-methylimidazolium chloride to reduce cellulose crystallinity. Compared to ball-milling IL pretreatment has several advantages: short pre-treatment times (1–3 h), IL reuse and the possibility to dissolve and immediately regenerate large quantities cellulose to its initial purity. IL selection was motivated by the efficiency of $Cl^-$ containing idazolium ILs in cellulose dissolution resulting from their high hydrogen bond basicity as well the low cost of this particular IL [41].

The highest sugar yield (74.5%, ball-milled cellulose substrate) reported for a solid acid catalyzed process is with CMK-3-$SO_3H$, an ordered mesoporous sulfonated carbon catalyst involving multi step synthesis [36]. Although the materials reported here did not outperform the CMK-3 catalyst, the 46–53 mol-C% yield obtained for P and J cake based materials were on a very high side especially considering their easy preparation, superiority over many other sulfonated catalysts, glucose selectivity and the ability to convert lignocellulosic biomass (Table 4) [42]. Further, there exists scope for improvement of sugar yield with optimization of reaction parameters, pretreatment conditions etc. Herein, the inferior saccharification activity of M cake based catalyst, MACS was due to formation of degradation products which was favored by inadequate adsorption of glucans due to slightly smaller pores, lack of weakly acidic sites and the high —$SO_3H$ density (Fig. 9). Further investigation with respect to reaction temperature showed 150 °C to be the optimum reaction temperature as degradation of glucose to HMF and Levulinic acid became prominent at higher reaction temperatures [42], while typical reaction time of 12–24 h was required to attain maximum glucose yield (Fig. 9). However, when reusability studies were performed with spent JACS, glucose yield increase from 51 to 61 mol-C%, which is most likely due to the inclusion of unreacted cellulose particles of previous run in the reactor. It results from the difficulties associated with absolute separation of the spent catalyst and unreacted cellulose particles, causing glucose overestimation in the successive run. This issue was recently addressed by Zhang et al. [43] with magnetic $Fe_3O_4$@C-$SO_3H$ catalyst at the expense of catalyst activity. Thus, our results corroborate the potential of DOWC derived sulfated mesoporous AC as effective solid catalysts for selectively hydrolyzing amorphous cellulose and lignocellulosic materials to sugars.

### 3.2.2. Oleic acid esterification

Fatty acid esterification is another important step in biorefining which converts the long fatty acids such as oleic acid (OA) present in vegetable oils to FAME (biodiesel). To investigate the prospective of the DOWC derived materials as biodiesel catalysts esterification was used as a model reaction. In contrast to cellulose saccharification, esterification is a much straightforward and less energy intensive process. Nonetheless, it involves large fatty acid molecules with typical kinetic diameter in the order of 2–2.4 nm. Thus, catalysts with large mesopores and specific surface area are expected to be more efficient in converting molecules like OA. Besides, esterification is a highly reversible equilibrium reaction requiring use of catalyst, excess alcohol and/or continuous $H_2O$ removal to get higher ester yields [44].

Fig. 10 shows a summary of the esterification activity of the different DOWC based sulfated carbons in comparison to $H_2SO_4$ and selected zeolites. The results clearly illustrate the catalytic superiority of the sulfonated materials in comparison to $H_2SO_4$, zeolites, non-sulfated materials and also point to the occurrence of a clear relation between catalyst structure (porosity, pore size, surface area etc.) and —$SO_3H$ density with ester yield, as also

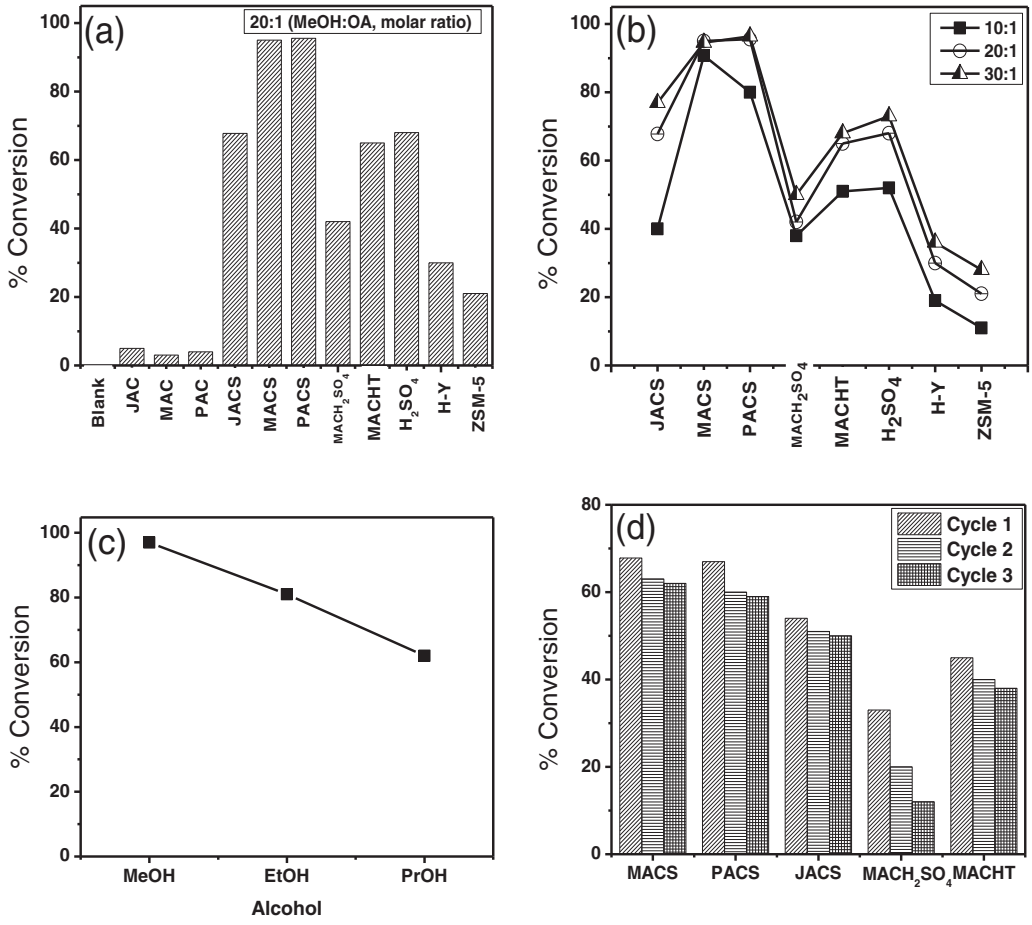


**Fig. 10.** Esterification activity of the DOWC biomass derived catalytic materials (a) comparison with 98% $H_2SO_4$, zeolites and the non-sulfated forms (investigated at 20:1) (b) effect of methanol to oleic acid molar ratio (c) alcohol chain length (shown for MACS at 30:1) and (d) reusability (3 h reaction). Reaction conditions: catalyst loading = 3 wt% of acid or 0.02 g $H_2SO_4$ (equivalent to —$SO_3H$ in MACS), $t$ = 10 h and $T$ = 64 °C.

reported by Yu et al. [11] and Kastner et al. [34] for biochar based sulfonated carbons. Here, the negligible conversion levels achieved with non-sulfated materials were consistent with the non-catalytic effects of weakly acidic —COOH, —OH and phosphate groups [4,34]. As expected, the highest acid conversion were obtained with the most porous PACS and MACS with relatively high —$SO_3H$ density of 0.75–0.84 mmol/$g_{cat}$ followed by the slightly less porous and acidic JACS (—$SO_3H$ density of 0.70 mmol/$g_{cat}$). On the other hand, the lower conversion obtained for MACHT could be attributed to its non-porous structure limiting accessibility of large OA [11,35] substrate to the active sites. While, the even lower conversion recorded for the conc. $H_2SO_4$ treated sulfonated catalyst, $MACH_2SO_4$ was attributed to its very low active site (—$SO_3H$) density (Table 3). Here, the insignificant catalytic effects of zeolites upon OA esterification is attributed to the limiting effects of pore space, surface acid site density as well as the lack of strong enough acid sites. Although, increasing the methanol concentration observably increased conversion level for the less active JACS, $MACH_2SO_4$ and MACHT, yet it didnot approach the levels achieved by MACS or PACS, Fig. 10(b). Overall, the order of esterification activity of the sulfated catalysts based on OA conversion was PACS = MACS > JACS > MACHT > $H_2SO_4$ > $MACH_2SO_4$, following a combined effect of acidity and porosity. The effects of alcohol chain length on conversion were also studied by repeating similar experiments with ethanol and 1-propanaol with MACS as a reference catalyst. The conversion achieved with ethanol was only 80% and it reduced even further to 62% with 1-propanol, Fig. 10(c) which could be explained on the basis of difference in reactivities of alcohols of different carbon chain lengths. Further, in terms of stability the catalysts obtained by method 1 also outperformed those obtained by methods 2 and 3. The poor reusability in the later were accounted with the easy leaching of —$SO_3H$ groups compared to the catalyst obtained by method 1 (Fig. 10(d), Table 3 and supporting information), Yu et al. [11] found a similar effect in sulfonated activated biochar catalysts obtained by $H_2SO_4$ treatment.

To further fortify the viability of these biodiesel waste derived materials as catalysts in biodiesel production, the TOF values were compared to the previously reported sulfonated catalysts (Table 5). As expected the TOF of the optimum, radically sulfonated AC (PACS and MACS) catalysts were higher than the hydrothermal and directly sulfonated AC (methods 2 and 3) as well as the sulfonated activated biochar (Kastner et al. [34]), sulfonated AC (commercial), sulfonated OMCs and Amberlyst-15 (Geng et al. [20]) demonstrating their catalytic superiority and in good agreement with the effects of catalyst —$SO_3H$ density and porosity (Table 5). However, the TOF of sulfonated starbon-300 (Aldana-Pérez et al. [9]) were even higher (~5 times the best DOWC catalyst) which could be attributed to the presence of extremely larger mesopores (average pore diameter >14 nm) and higher —$SO_3H$ density. In contrast, the DOWC based catalysts reported here possessed a mixed texture with average pore diameter 3.9–4.9 nm; thus, the possibility of steric effect due to agglomeration of OA molecules at pore mouth were higher in the DOWC based catalysts compared to the sulfonated starbon-300 catalyst with very large pores [44]. Overall esterification activities of the mesoporous DOWC catalyst obtained by method 1 were higher than ion exchange resins (Amberlyst-15)

**Table 5**
Comparison of the esterification activity of the DOWC derived sulfonated carbons with reported sulfonated catalysts.

| Catalyst | Raw material(Carbon source) | Sulfonating agent | $T$ °C | Methanol-oil (molar ratio) | $V_p$ $cm^3/g$ | $S_{BET}$ $m^2/g$ | —$SO_3H$ density mmol/g | TOF $h^{-1}$ | TOF $min^{-1}$ | Refs. |
|---|---|---|---|---|---|---|---|---|---|---|
| JACS | J DOWC | 4-BDS | 64 | 20 | 0.23 | 96 | 0.70 | 70.81 | 1.18 | This |
| PACS | P DOWC | 4-BDS | 64 | 20 | 0.46 | 483 | 0.84 | 104 | 1.733 | work, |
| MACS | M DOWC | 4-BDS | 64 | 20 | 0.41 | 468 | 0.75 | 102.3 | 1.705 | [a][25] |
| [a], MAC-$SO_3H$ | M DOWC | 4-BDS | 80 | 21 | n.r. | 556 | 0.73 | 51.5 | 0.854 | |
| MACHT | M DOWC | $H_2SO_4$ | 64 | 20 | 0.03 | <1 | [a]1.30 | 29.2 | 0.486 | |
| MACH$_2SO_4$ | M DOWC | $H_2SO_4$ | 64 | 20 | 0.61 | 690 | [a]0.30 | 26 | 0.433 | |
| AgForm-400C-SO4 | AgForm 400 biochar | $H_2SO_4$ | 47 | 20 | 0.0005 | 338 | 0.45 ± 0.03 | – | 0.04 | [34] |
| PHC-400C-SO4 | Peanut hull char | $H_2SO_4$ | 57 | 20 | 0.13 | 242 | 0.61 ± 0.03 | – | 0.15 | [34] |
| WVB-20-SO4 | Wood AC | $H_2SO_4$ | 57 | 20 | 0.76 | 1391 | 0.2 ± 0.01 | – | 0.18 | [34] |
| BX-7540-SO4 | Wood AC | $H_2SO_4$ | 60 | 20 | 0.34 | 967 | 0.1 ± 0.002 | – | 0.56 | [34] |
| WVB-20-SO3 | Wood AC | $SO_3$ | 60 | 20 | 0.63 | 1137 | 0.81 ± 0.01 | – | 0.18 | [34] |
| SC-CCA3 | Resorcinol resin, γ-$Al_2O_3$ | 4-BDS | 65 | 57 | 0.57 | 623 | 1.70 | 102 | – | [20] |
| Starbons-300A2 | Starbon-300 | $ClSO_3H/H_2SO_4$ | 80 | 10 | – | 75 | 1.80 | 509[b] | – | [9] |
| S-AC | mesoporous AC | 4-BDS | 65 | 57 | 0.24 | 318 | 1.42 | 44 | – | [20] |
| Amberlyst-15 | – | – | 65 | 57 | 0.31 | 43 | 5.03 | 15 | – | [20] |

[a] =(—$SO_3H$ + —SH).
[b] Activity/mmol—$SO_3H$.

and the sulfonated (biochar, commercial AC, OMCs and carbohydrate), confirming potential of the waste derived solid acids as environmentally benign integrated catalysts for biodiesel production.

## 4. Conclusions

In summary, herein, we report an efficient technique for the valorization of solid wastes generated from biodiesel production into highly active mesoporous sulfonated carbon catalysts. These abundant wastes are promising source for in situ preparation of solid acid catalysts, an important step towards the realization of competitive, carbon efficient biorefineries. These waste derived materials exhibited high catalytic activity in amorphous cellulose saccharification (glucose yield upto 53%) and fatty acid esterification (conversion upto 97%) outperforming $H_2SO_4$, traditional solid acids and several sulfonated catalysts reported earlier. Structurally these multifunctional solid acids are more complex than carbohydrate, sugar and resin based sulfonated carbons reported previously and in addition to the normally found —$SO_3H$, —COOH and —OH groups carbons they contain several N (and phosphate, when activated by phosphoric acid) groups incorporated into their structural frameworks. Further, the structures, stability, textural and catalytic properties of these materials were directly affected by the preparation method (activation, sulfonating agent) and raw material properties and the best catalysts with mesoporous structure (average pore diameter 3.9–4.8 nm, pore volume 0.28–0.46 $cm^3\ g^{-1}$) and —$SO_3H$ density (0.7–0.84 $mmol/g_{cat}$) were obtained by 4-BDS sulfonation of chemically activated DOWC biomass.

## Acknowledgments

Centre for International Mobility – CIMO (Finland) is acknowledged for providing visiting doctoral fellowship to Lakhya Jyoti Konwar at Åbo Akademi University. This work is part of the activities at the Åbo Akademi Process Chemistry Centre (ÅA-PCC) within the Centre of Excellence Programme appointed by Åbo Akademi University. Dr. Andrey Shchukarev, Department of Chemistry Umeå University (Sweden) is acknowledged for his valuable help with XPS analysis. SAIF, North East Hill University, Shillong (India) is acknowledged for TEM analysis. The authors also acknowledge L. Silvander, ÅA-PCC for EDX analysis.

## Appendix A. Supplementary data

Supplementary data associated with this article can be found, in the online version, at http://dx.doi.org/10.1016/j.apcatb.2015.03.005.

## References

[1] S. Zheng, M. Kates, M.A. Dubé, D.D. McLean, Acid-catalyzed production of biodiesel from waste frying oil, Biomass Bioenergy 30 (3) (2006) 267–272.
[2] A. Hoogendoorn, H. van Kasteren, Transportation biofuels: novel pathways for the production of ethanol, in: J.H. Clark, G.A. Kraus (Eds.), Biogas and Biodiesel, Royal Society of Chemistry, 2010.
[3] L.J. Konwar, J. Boro, D. Deka, Review on latest developments in biodiesel production using carbon-based catalysts, Renew. Sustain. Energy Rev. 29 (2014) 546–564.
[4] M. Hara, T. Yoshida, A. Takagaki, T. Takata, J.N. Kondo, S. Hayashi, K. Domen, Biomass conversion by a solid acid catalyst, Energy Environ. Sci. 3 (2010) 601–607.
[5] M. Okamura, A. Takagaki, M. Toda, J.N. Kondo, K. Domen, T. Tatsumi, M. Hara, S. Hayashi, Acid-catalyzed reactions on flexible polycyclic aromatic carbon in amorphous carbon, Chem. Mater. 18 (2006) 3039–3045.
[6] M. Gonçalves, V.C. Souza, T.S. Galhardo, M. Mantovani, F.C.A. Figueiredo, D. Mandelli, W.A. Carvalho, Glycerol conversion catalyzed by carbons prepared from agroindustrial wastes, Ind. Eng. Chem. Res. 52 (2013) 2832–2839.
[7] L. Peng, A. Philippaerts, X. Ke, J. Van Noyen, F. De Clippel, G. Van Tendeloo, P.A. Jacobs, B.F. Sels, Preparation of sulfonated ordered mesoporous carbon and its use for the esterification of fatty acids, Catal. Today 150 (2010) 140–146.
[8] M.H. Zong, Z.Q. Duan, W.Y. Lou, T.J. Smith, H. Wu, Preparation of a sugar catalyst and its use for highly efficient production of biodiesel, Green Chem. 7 (2007) 434–437.
[9] A. Aldana-Pérez, L. Lartundo-Rojas, R. Gómez, M.E. Niño-Gómez, Sulfonic groups anchored on mesoporous carbon Starbons-300 and its use for the esterification of oleic acid, Fuel 100 (2012) 128–138.
[10] B.L.A.P. Devi, K.N. Gangadhar, P.S.S. Prasad, B. Jagannadh, R.B.N. Prasad, Glycerol-based carbon catalyst for the preparation of biodiesel, ChemSusChem 2 (7) (2009) 617–620.
[11] J.T. Yu, A.M. Dehkhoda, N. Ellis, Development of biochar-based catalyst for transesterification of canola oil, Energy Fuels 25 (2010) 337–344.
[12] M. Kitano, K. Arai, A. Kodama, T. Kousaka, K. Nakajima, S. Hayashi, M. Hara, Preparation of a sulfonated porous carbon catalyst with high specific surface area, Catal. Lett. 131 (2009) 242–249.
[13] Q. Shu, J. Gao, Z. Nawaz, Y. Liao, D. Wang, J. Wang, Synthesis of biodiesel from waste vegetable oil with large amounts of free fatty acids using a carbon-based solid acid catalyst, Appl. Energy 87 (8) (2010) 2589–2596.
[14] B.V.S.K. Rao, K.C. Mouli, N. Rambabu, A.K. Dalai, R.B.N. Prasad, Carbon-based solid acid catalyst from de-oiled canola meal for biodiesel production, Catal. Commun. 14 (2011) 20–26.
[15] R.A. Arancon, H.R. Barros Jr., A.M. Balu, C. Vargas, R. Luque, Valorisation of corncob residues to functionalised porous carbonaceous materials for the simultaneous esterification/transesterification of waste oils, Green Chem. 13 (2011) 3162–3167.
[16] B. Chang, J. Fu, Y. Tian, X. Dong, Soft-template synthesis of sulfonated mesoporous carbon with high catalytic activity for biodiesel production, RSC Adv. 3 (2013) 1987–1994.

[17] V.V. Ordomsky, J.C. Schouten, J. van der Schaaf, T.A. Nijhuis, Foam supported sulfonated polystyrene as a new acidic material for catalytic reactions, Chem. Eng. J. 207–208 (2012) 218–225.
[18] J. Ji, G. Zhang, H. Chen, S. Wang, G. Zhang, F. Zhang, X. Fan, Sulfonated graphene as water-tolerant solid acid catalyst, Chem. Sci. 2 (2011) 484–487.
[19] R. Liu, X. Wang, X. Zhao, P. Feng, Sulfonated ordered mesoporous carbon for catalytic preparation of biodiesel, Carbon 46 (2008) 1664–1669.
[20] L. Geng, Y. Wang, G. Yu, Y. Zhu, Efficient carbon-based solid acid catalysts for the esterification of oleic acid, Catal. Commun. 13 (2011) 26–30.
[21] M. Verma, S. Pradhan, S. Sharma, S.N. Naik, R. Prasad, Efficacy of karanjin and phorbol ester fraction against termites (*Odontotermes obesus*), Int. Biodeterior. Biodegrad. 65 (2011) 877–882.
[22] F. Deeba, V. Kumar, K. Gautam, R.K. Saxena, D.K. Sharma, Bioprocessing of *Jatropha curcas* seed oil and deoiled seed hulls for the production of biodiesel and biogas, Biomass Bioenergy 40 (2012) 13–18.
[23] A. Maarten, J. Kootstra, H.H. Beeftink, J.P.M. Sanders, Valorisation of *Jatropha curcas*: solubilization of proteins and sugars from the NaOH extracted de-oiled press cake, Ind. Crops Prod. 34 (1) (2011) 972–978.
[24] T. Vernersson, P.R. Bonelli, E.G. Cerrella, A.L. Cukierman, *Arundo donax* cane as a precursor for activated carbons preparation by phosphoric acid activation *Arundo donax* cane as a precursor for activated carbons preparation by phosphoric acid activation, Bioresour. Technol. 83 (2002) 95–104.
[25] L.J. Konwar, R. Das, A.J. Thakur, E. Salminen, P. Mäki-Arvela, N. Kumar, J.P. Mikkola, D. Deka, Biodiesel production from acid oils using sulfonated carbon catalyst derived from oil-cake waste, J. Mol. Catal. A Chem. 388–389 (2014) 167–176.
[26] B. Zhang, J. Ren, X. Liu, Y. Guo, Y. Guo, G. Lu, Y. Wang, Novel sulfonated carbonaceous materials from *p*-toluenesulfonic acid/glucose as a high-performance solid-acid catalyst, Catal. Commun. 11 (2010) 629–632.
[27] A. Onda, T. Ochi, K. Yanagisawa, Hydrolysis of cellulose selectively into glucose over sulfonated activated-carbon catalyst under hydrothermal conditions, Top. Catal. 52 (2009) 801–807.
[28] J.K. Satyarthi, D. Srinivas, P. Ratnasamy, Estimation of free fatty acid content in oils, fats, and biodiesel by $^{1}$H NMR spectroscopy, Energy Fuels 23 (2009) 2273–2277.
[29] A.M. Puziy, O.I. Poddubnaya, A. Martinez-Alonso, F. Suarez-Garc, J.M.D. Tascon, Synthetic carbons activated with phosphoric acid – I. Surface chemistry and ion binding properties, Carbon 40 (2002) 1493–1505.
[30] J. Wei, P. Hing, Z.Q. Mo, TEM, XPS and FTIR characterization of sputtered carbon nitride films, Surf. Interface Anal. 28 (1999) 208–211.
[31] A.M. Puziya, O.I. Poddubnayaa, R.P. Sochab, J. Gurgulb, M. Wisniewskic, XPS and NMR studies of phosphoric acid activated carbons, Carbon 46 (15) (2008) 2113–2123.
[32] T.C. Nagaiah, A. Bordoloi, M.D. Sanchez, M. Muhler, W. Schuhmann, Mesoporous nitrogen-rich carbon materials as catalysts for the oxygen reduction reaction in alkaline solution, ChemSusChem 5 (2012) 637–641.
[33] A.C. Ferrari, J. Robertson, Interpretation of Raman spectra of disordered and amorphous carbon, Phys. Rev. B Condens. Matter 61 (20) (2000) 14095–14107.
[34] J.R. Kastner, J. Millera, D.P. Geller, J. Locklin, L.H. Keith, T. Johnson, Catalytic esterification of fatty acids using solid acid catalysts generated from biochar and activated carbon, Catal. Today 190 (2012) 122–132.
[35] M.J. Climent, A. Corma, S. Iborra, Conversion of biomass platform molecules into fuel additives and liquid hydrocarbon fuels, Green Chem. 16 (2014) 516–547.
[36] J. Pang, A. Wang, M. Zheng, T. Zhang, Hydrolysis of cellulose into glucose over carbons sulfonated at elevated temperatures, Chem. Commun. 46 (2010) 6935–6937.
[37] M. Kitano, D. Yamaguchi, S. Suganuma, K. Nakajima, H. Kato, S. Hayashi, M. Hara, Adsorption-β-1,4 glucans on graphene-based amorphous carbon bearing $SO_3H$, COOH, and OH groups, Langmuir 25 (2009) 5068–5075.
[38] S.V. de Vyver, L. Peng, J. Geboers, H. Schepers, F. de Clippel, C.J. Gommes, B. Goderis, P.A. Jacobs, B.F. Sels, Sulfonated silica/carbon nanocomposites as novel catalysts for hydrolysis of cellulose to glucose, Green Chem. 12 (2010) 1560–1563.
[39] J. Pang, A. Wang, M. Zhenga, T. Zhang, Hydrolysis of cellulose into glucose over carbons sulfonated at elevated temperatures, Chem. Commun. 46 (2010) 6935–6937.
[40] Y. Yu, H. Wu, Effect of ball milling on the hydrolysis of microcrystalline cellulose in hot-compressed water, AIChE J. 57 (3) (2011) 793–800.
[41] P. Mäki-Arvela, I. Anugwom, P. Virtanen, R. Sjöholm, J.P. Mikkola, Dissolution of lignocellulosic materials and its constituents using ionic liquids—a review, Ind. Crops Prod. 32 (2010) 175–201.
[42] S. Larsson, E. Palmqvist, B. Hahn-Hägerdal, C. Tengborg, K. Stenberg, G. Zacchi, N. Nilvebrant, The generation of fermentation inhibitors during dilute acid hydrolysis of softwood, Enzyme Microb. Technol. 24 (3–4) (1999) 151–159.
[43] C. Zhang, H. Wang, F. Liu, L. Wang, H. He, Magnetic core–shell $Fe_3O_4$@C–$SO_3H$ nanoparticle catalyst for hydrolysis of cellulose, Cellulose 20 (2013) 127–134.
[44] A.C. Carmo Jr., L.K.C. de Souza, C.E.F. da Costa, E. Longo, J.R. Zamian, G.N. da Rocha Filho, Production of biodiesel by esterification of palmitic acid over mesoporous aluminosilicate Al-MCM-41, Fuel 88 (3) (2009) 461–468.